CRCLEME
Cooperative Research Centre for
Landscape Evolution & Mineral Exploration

OPEN FILE
REPORT
SERIES

GEOCHEMICAL ORIENTATION SOIL-LAG TRAVERSE AT THE GARLAND GOLD MINE, WINNECKE GOLDFIELD, NORTHERN TERRITORY

M.S. Skwarnecki and S.J. Fraser

CRC LEME OPEN FILE REPORT 83

January 2002

(CSIRO Exploration and Mining Report 740R/CRC LEME Report 144R, 2000.
Second impression 2002)

CRCLEME
Cooperative Research Centre for
Landscape Evolution & Mineral Exploration

GEOCHEMICAL ORIENTATION SOIL-LAG TRAVERSE AT THE GARLAND GOLD MINE, WINNECKE GOLDFIELD, NORTHERN TERRITORY

M.S. Skwarnecki and S.J. Fraser

CRC LEME OPEN FILE REPORT 83

January 2002

(CSIRO Exploration and Mining Report 740R/CRC LEME Report 144R, 2000.
Second impression 2002)

CRC LEME is an unincorporated joint venture between CSIRO-Exploration & Mining, and Land & Water, The Australian National University, Curtin University of Technology, University of Adelaide, University of Canberra, Geoscience Australia, Bureau of Rural Sciences, Primary Industries and Resources SA, NSW Department of Mineral Resources-Geological Survey and Minerals Council of Australia.
Headquarters: CRC LEME c/o CSIRO Exploration and Mining, PO Box 1130, Bentley WA 6102, Australia

This report presents outcomes of research by CRC LEME for Gutnick Resources NL as support for their search for Witwatersrand style Au deposits in the Ngalia and Amadeus basins,, Northern Territory. The Project was commenced in April 1999, concluded in 2000 and was led by Dr I.D.M. Robertson. Agreement was reached between Gutnick Resources NL and CRC LEME on 19th December 2001 to release CRC LEME Reports 144R, 148R and 149R into the public domain through the CRC LEME Open File Report series. It is intended that publication of the reports will be an additional factor in transferring technology to aid the Australian mineral industry.

This report (CRC LEME Open File Report 83) is a second impression (second printing) of CSIRO Exploration and Mining Restricted Report 740R / CRC LEME Report 144R, first issued in 2000.

Copies of this publication can be obtained from:
The Publication Officer, c/- CRC LEME, CSIRO Exploration and Mining, P.O. Box 1130, Bentley, WA 6102, Australia. Information on other publications in this series may be obtained from the above or from http://leme.anu.edu.au/

Cataloguing-in-Publication:
Skwarnecki, M.S.
Geochemical orientation soil-lag traverse at the Garland Gold Mine, Winnecke Goldfield, Northern Territory
ISBN 0 643 06776 0
1. Geochemistry 2. Gold - Northern Territory - Winnecke 3. Soils - Northern Territory - Winnecke
I. Fraser, S.J. II. Title
CRC LEME Open File Report 83.
ISSN 1329-4768

Addresses of authors

M. Skwarnecki
Cooperative Research Centre for Landscape Evolution and Mineral Exploration
c/- CSIRO Land and Water
Private Mail Bag 2
Glen Osmond SA 5064
Australia

S.J. Fraser
CSIRO Exploration and Mining
QCAT, P.O. Box 883
Kenmore,
QLD 4069
Australia

PREFACE AND EXECUTIVE SUMMARY

This report is part of CRC LEME's final documentation of input to the Rand Project for Gutnick Resources. It was designed to assist Gutnick Resources in their search for Witwatersrand-style gold deposits in the Amadeus and Ngalia basins in the Northern Territory. This could be facilitated if the influence of the regolith was understood, ensuring correct exploration strategies, sample media and data interpretation methods. The project began in February 1998 and was terminated in February 1999. The principal objectives were:-

- To map and characterise the regolith within the Amadeus and Ngalia basins at reconnaissance and local scales and to understand its development.
- To translate this into sampling and exploration strategies.

Part of the latter objective was to complete orientation work at Garland and Edwards Creek to guide future sampling. This report covers the Garland orientation survey.

Basic knowledge of the geochemical behaviour of pathfinder elements is critical to the determination of a relevant element suite, design of sampling programmes and, ultimately, exploration success. The report illustrates the need to conduct meaningful geochemical orientation surveys, particularly in those regions that have not received much 'modern' exploration. At Garland, elements associated with mineralisation partition into two main size fractions, namely Au, Bi and W into the coarse fractions, and Au, Cu, Hg, S and Sb into the fine. Without this simple recognition, collection of the appropriate size fraction(s) and identification of the geochemical signature of the mineralisation are likely to be fortuitous. There is no significant relationship between Au and Ca so it is unlikely that the regolith carbonates are pedogenic and calcrete sampling may be inappropriate in this region.

I.D.M. Robertson
Project Leader

CONTENTS

LIST OF FIGURES

LIST OF APPENDICES

ABSTRACT

Gold mineralisation at the Garland Mine, Winnecke Goldfield, occurs in a series of east-striking lodes (zones of silicification) in a north-striking corridor, hosted by quartz-mica±feldspar schists. Nine soil-lag samples were collected along a traverse 180 m in length across the corridor of mineralisation. The lag consisted dominantly of siliceous lode, quartz fragments and hematitic silcrete, except at the eastern and western extremities of the traverse, where quartz-mica±feldspar lag is relatively common. Calcrete also occurs and is mainly restricted to the area along strike from the old workings.

Seven size fractions (bulk <6 mm, 6-2 mm, 2-1 mm, 1-0.5 mm, 0.5-0.25 mm, 0.25 mm-75µm, and <75 µm) for each sample site were analysed for Ag, As, Au, Bi, Ca, Cr, Cu, Fe, Hg, K, Mg, Mn, Mo, Na, Ni, Pb, Rb, S, Sb, Sn, Te, U, W, and Zn. This was by ICP-MS and ICP-OES, following mixed acid digest (except Au and Hg: dissolution in aqua regia).

The mineralised zone is characterised by anomalous As, Au, Bi, Cu, Hg, S, Sb and W. The best responses for Bi and W are given by the coarsest fraction (6-2 mm), whereas for Cu, Hg, S and Sb, the best fraction is the finest (<75 µm). For Au, the best response is in the <75 µm fraction, although there is also a response in the 6-2 mm fraction. For As, the response is very similar for all fractions.

The results indicate that the best overall responses are for the intermediate and fine fractions (commonly the <75 µm fraction), although a compromise would be the <2 mm fraction, simplifying sample collection. However, there is a significant response in the 6-2 mm fraction for Au, Bi and W. This fraction could also be used, but further work would be required.

There is no significant relationship between Au and Ca so it is unlikely that the regolith carbonates are pedogenic and calcrete sampling may be inappropriate in this region.

1. INTRODUCTION

1.1 Location

The Winnecke Goldfield is located about 70 km northeast of Alice Springs (Figure 1), and forms an east-west belt extending for about 15 km. The Garland workings occur in the eastern part of the field (Figure 2) at 23°20'11"S and 134°22'44"E.

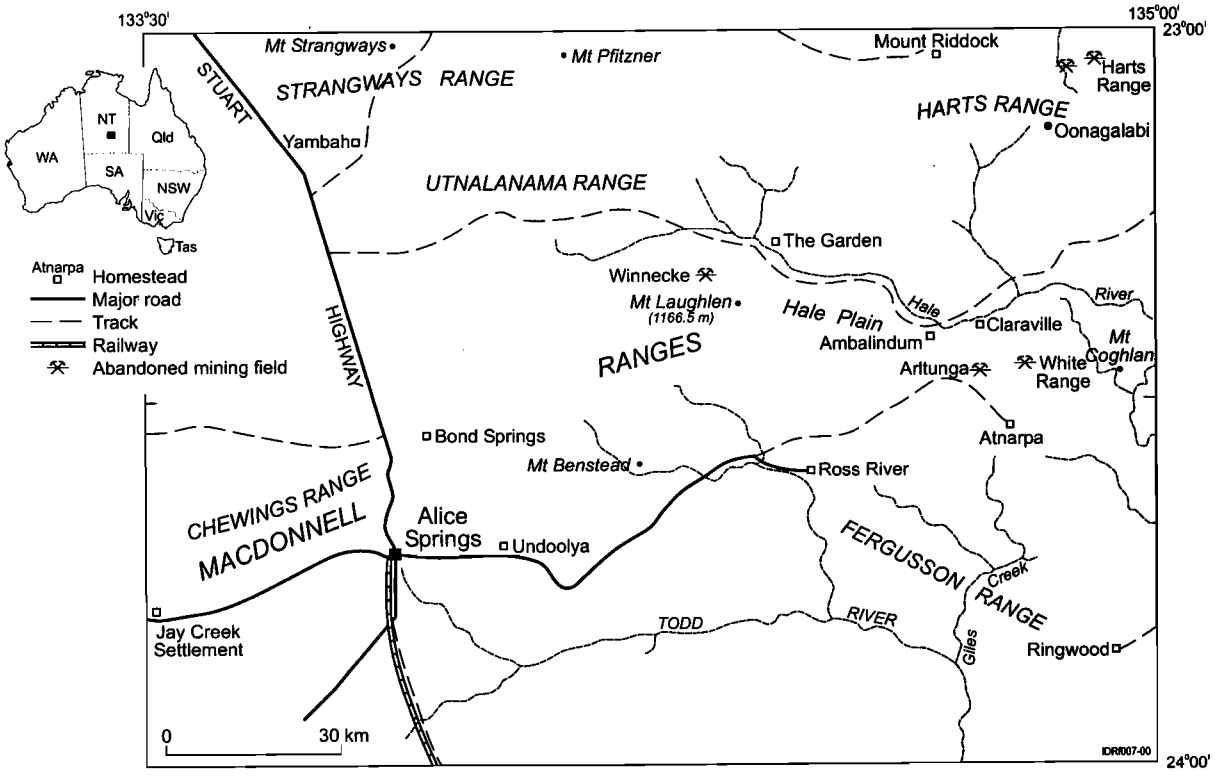

Figure 1. Location map of the Winnecke Goldfield.

1.2 Objectives

The objectives of the soil-lag orientation traverse were to:

(i) determine the geochemical signature of the mineralisation;
(ii) establish the best sampling procedure.

The site was chosen principally because there appears to be little evidence for contamination around the old workings (in contrast to the nearby Golden Goose Mine; Skwarnecki et al., 2000), and there has been previous documentation of the geology of the mine.

2. REGIONAL GEOLOGICAL SETTING

The Winnecke Goldfield straddles the structural contact between the Palaeoproterozoic Arunta Province and the basal Neoproterozoic sequence of the Amadeus Basin (Figure 2). The Arunta Province rocks belong to several distinct units of Divisions One and Two of the Central Zone (Shaw and Langworthy, 1984). These are: -

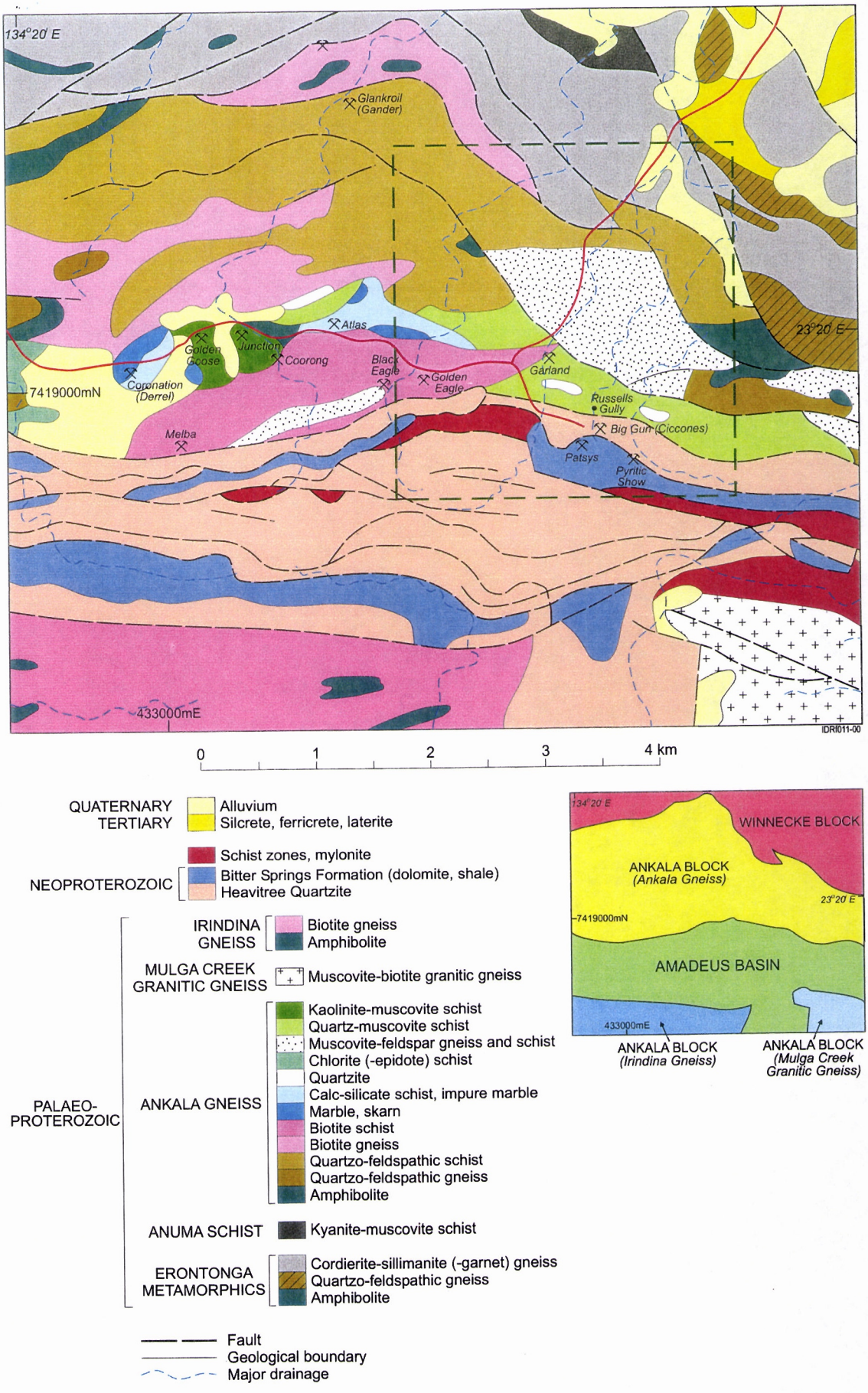

Figure 2. Generalised geological map of the Winnecke Goldfield (after Pigott, 1984) showing the location of the Garland Prospect. The dashed outline corresponds to the detailed regolith map of Figure 5.

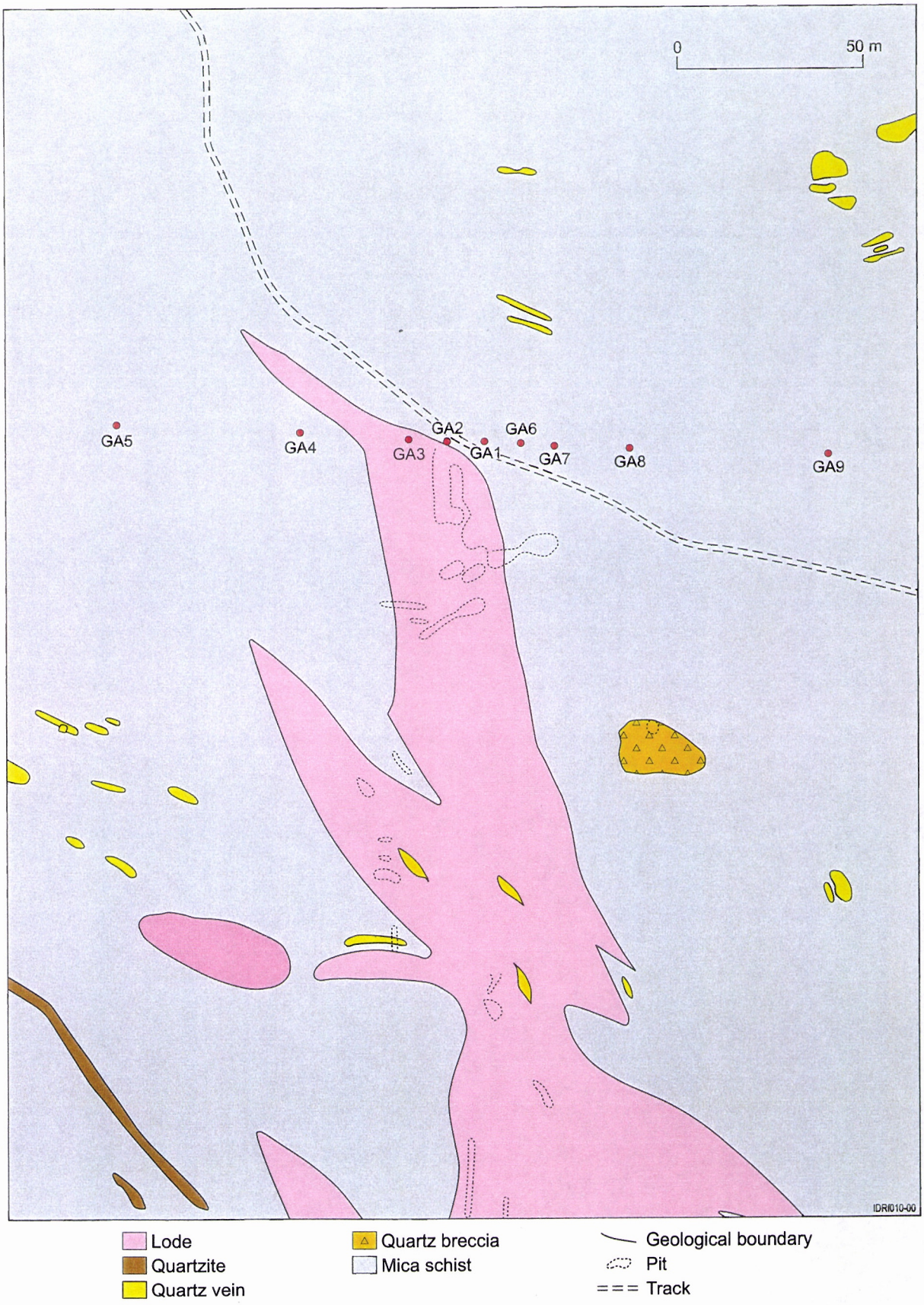

Figure 3. Geological map of the Garland mine showing location of sample sites.

(i) the *Erotonga Metamorphics* (cordierite-, garnet- and sillimanite-bearing gneisses, locally with calc-silicate and amphibolite horizons) and the *Anuma Schist* (staurolite- kyanite- and mica-bearing schists and gneisses), forming the Winnecke Block (Division One lithologies);

(ii) Ankala Gneiss (biotitic schists and gneisses, calc-silicates and marbles, quartzo-feldspathic gneisses and amphibolites), forming part of the Ankala Block (Division Two lithologies) north of the Amadeus Basin rocks;

(iii) Irindina Gneiss (quartzo-feldspathic gneisses, biotite schists and amphibolites) forming part of the Ankala Block;

(iv) the Mulga Creek Granitic Gneiss (muscovite-biotite granitic gneiss and minor amphibolite), forming part of the Ankala Block.

The overall metamorphic grade is upper amphibolite facies. However, retrograde greenschist facies rocks occur within schist zones, which are related to faulting and thrusting along deformation zones within the Arltunga Nappe Complex during the Devonian/Carboniferous Alice Springs Orogeny (Forman, 1971).

The *Heavitree Quartzite* (quartzites with grits and conglomerates) and the *Bitter Springs Formation* (shales and dolomites) represent the basal sequence of the Amadeus Basin. These units unconformably overlie Arunta Province rocks at Mt Laughlen (Joklik, 1955), to the south of Winnecke, but have been thrust over the Arunta Province rocks to the north, in the Winnecke area, where they are strongly deformed.

The Winnecke gold deposits occur in greenschist retrograde schist zones (Shaw and Langworthy, 1984), mainly within rocks of the Arunta Province. The dominant type of mineralisation (Wygralak and Bajwah, 1998) is auriferous quartz veining, with gold concentrated in those portions of the quartz veins that are composed of cellular and limonitic quartz, the limonite being derived from the oxidation of pyrite which occurs at depth.

Figure 4. General view of the old Garland workings, with the ridge of ferruginous and siliceous lode in the background. Note the coarse-grained siliceous lag, derived from the lode horizon and quartz veinlets therein, in the foreground.

3. GEOLOGY OF THE GARLAND MINE

Quartz-biotite-muscovite±feldspar schists are the dominant lithology (Figure 3; D.M. Ransom, in Clarke, 1971); other lithologies include marble and minor, pale blue quartzite. The foliation (parallel to lithological layering) dips 30-50°N, except in the hinges of small folds. The lode comprises a fine-grained, ferruginous quartz rock (i.e., a ferruginous silicified zone; Figure 4) and may include quartz veins. There are two types of quartz veins:

(a) brecciated quartz veins, apparently restricted to the lode, comprising white quartz fragments cemented in a ferruginous and siliceous matrix; and
(b) white quartz veins, cross-cutting foliation in the schists, and apparently unmineralised.

The lode occurs as a series of east-striking lenses, dipping at 30-35°N (D.M. Ransom, in Clarke, 1971) within a zone trending approximately north. The lode horizon forms a series of ridges.

Hossfeld (1940) described the Garland workings and stated that a rich pocket yielded over 300 oz (over 9 kg) of Au from a small outcrop of limonitic material at the northern end of a north-trending ironstone ridge. He suggested that the occurrence was probably due to strong secondary enrichment, because an adit driven into the ridge 15 feet (4.57 m) below the occurrence failed to intersect 'a continuation of the shoot'. Sampling of the adit offered little encouragement, apart from one assay of 2.91 ppm Au from 'fractured quartz in friable schists' 10 feet (3.05 m) from the adit portal. On the southern side of the ridge, about 200 feet (60 m) from the main workings, a thin quartz-ironstone vein (with coarse, visible gold) yielded an assay of 46.2 ppm Au associated with minor copper staining. Elsewhere, grab samples of quartz breccia yielded results that varied from below the limit of detection to 4.6 ppm Au.

Production figures are uncertain, but over 3 kg Au are stated to have been produced (Wygralak, 1995), making the deposit the third highest producer at Winnecke.

Exploration of the area around the old mine in the late 1960's and early 1970's (Clarke, 1971) failed to generate any targets. Rock-chip sampling of the lode yielded only a few assays above detection limit, the highest being 0.3 ppm Au.

4. LOCAL REGOLITH GEOLOGY

The area (Figure 5) consists of a quartzite range to the south. Elsewhere there are low, rolling hills with outcrops of various schists (biotite, muscovite-biotite), gneisses (quartzo-feldspathic, cordierite, garnet, biotite), amphibolites, quartz veins and calc-silicate rocks covered by a thin, skeletal soil. These grade into pediments and undulating erosional plains with a veneer of lithic soil and a lag of lithic fragments on saprock. The pediments are being actively dissected. All this comprises an erosional landform regime. Depositional landforms are restricted to the environs of incised, narrow creeks beds and consist of colluvial pediments of lithic fragments and sheetwash detritus, some with a sandy or clay-rich soil. The Garland mine is on a low hill, where outcrops of siliceous lode, quartz veins and mica schist are common. The land surface is mantled by a well-developed lag surface derived from these lithologies, particularly the more durable siliceous materials.

5. SAMPLE COLLECTION AND PREPARATION

The soil-lag traverse was located along strike from a line of shallow pits along the crest of a north-striking ridge. The mid-point of the traverse (sample GA1) was collected along strike of a series of shallow pits on the ridge; it was assumed that these pits marked the zone of mineralisation. Nine samples (see Appendix 1) were collected over a distance of 180 m across strike of the north-trending silicified zone (Figure 3). Samples were collected at 10-20 m intervals close to mineralisation and 50 m intervals distant from it (80 m).

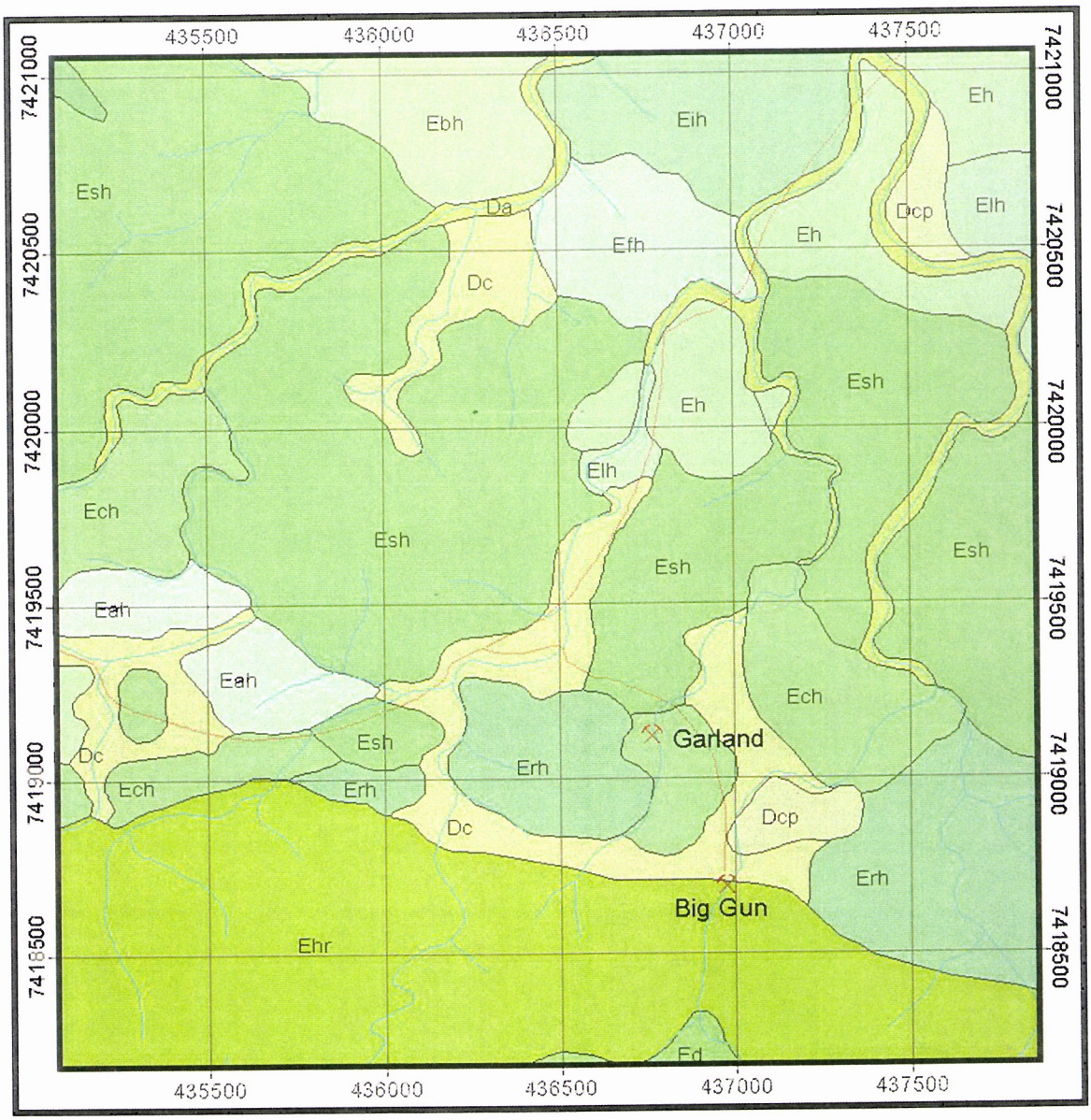

Figure 5. Regolith geology around the Garland Prospect (after Skwarnecki et al., 2000).

Lag was swept from the surface using a plastic brush and pan and about 0.3 kg of the 6-2 mm fraction was screened out (plastic and nylon sieves) and bagged on site. At the same site, soil was sampled from a shallow hole (to 20 cm depth) from which about 0.3 kg of bulk sample (<6 mm) and about 2 kg of <2 mm material were collected. The <2 mm fraction was further sieved in the laboratory (also using plastic/nylon sieves) into 2-1 mm, 1-0.5 mm, 0.5-0.25 mm, 0.25 mm-75 µm, and <75 µm fractions. A reference sample of each fraction was retained. A 100 g aliquot of each fraction was milled to <75 µm using a low-contamination K1045 ring mill (Robertson et al., 1996) with quartz washes between samples.

Soil pH was measured at each sample site using the soil pH test kit, developed by CSIRO and produced by Inoculo Laboratories in Melbourne.

6. GEOCHEMICAL ANALYSIS

6.1 Digestion and analysis

The milled aliquots were analysed in random order by inductively coupled plasma mass spectrometry (ICP-MS) and optical emission spectrometry (ICP-OES) by UltraTrace in Perth. The respective element suites were:

(i) Au, Hg: aqua regia digest (a mixture of nitric and hydrochloric acids) on a nominal 40 g sample, and analysis by ICP-MS;
(ii) ICP-MS suite (Ag, As, Bi, Mo, Pb, Rb, Sb, Se, Sn, Te, U, W): sample digestion with hydrochloric, nitric and hydrofluoric acids, with a final dissolution in hydrochloric acid (mixed acid digest);
(iii) ICP-OES suite (Ca, Cu, Cr, Fe, K, Mg, Mn, Na, Ni, S, Zn): sample digestion with hydrochloric, nitric and hydrofluoric acids, with a final dissolution in hydrochloric acid (mixed acid digest).

6.2 Quality control

Pulped in-house weathered rock reference materials (Standards 6 and 9) were placed into the analytical stream to monitor precision. The results are given in Appendix 3 and indicate that the replicate analyses are generally in good agreement with preferred values.

7. SOIL-LAG GEOCHEMISTRY

7.1 Background and peak concentrations

Background and peak values for the elements in each fraction (Table 1) were estimated from the graphs of element distributions along the traverse (Figure 6A-V). Sample populations are small, so the results should be treated with caution.

7.2 Lag lithologies

The dominant lag types present over most of the traverse comprise fragments of the lode horizon (silicified material), quartz vein fragments and fine-grained hematitic silcrete. Calcrete is relatively abundant at the mid-point of the traverse and for 20 m to the east, but occurs in significantly lesser amounts further east. Minor calcrete also occurs for about 20 m to the west of the mid-point. The presence of calcrete is reflected in the soil pH, which varies from 6 in the west (where calcrete was absent), to 7 (minor calcrete), to 9.5-10 where calcrete is abundant. A lag of quartz-muscovite-feldspar±biotite schist and quartz-biotite-feldspar schist (with or without vein quartz) occurs at the western and eastern ends of the traverse respectively .

Table 1.
Peak and background concentrations for mineralisation-associated elements for soils and lag, Garland mine

Element	Units	bulk <6 mm		6-2 mm		2-1 mm		1-0.5 mm		0.5-0.25 mm		0.25 mm-75 mm		< 75 mm	
		background	peak	background	peak	background	peak	background	peak	background	peak	background	peak	background	peak
As	ppm	1.5	5	1.5	6	1.5	5.5	2	5.5	2	5	1.5	4	2	5
Au	ppb	<1	147	<1	31	<1	82	<1	183	<1	120	<1	151	<1	218
Bi	ppm	0.6	1	0.6	1.6	0.6	1.5	0.5	0.9	0.5	0.9	0.5	0.8	0.6	0.8
Cu	ppm	20-25	42	15-22	31	15-25	42	15-28	42	18-30	43	15-26	38	19-32	43
Hg	ppb	25	60	10	40	10	40	10	50	10	40	10	40	20	60
S	ppm	50-80	300	45	200	70-110	240	60-100	220	60-80	200	60-75	200	100-110	300
Sb	ppm	0.6	5.6	0.4	4.6	0.6	6.8	0.6	4.8	0.6	4.6	0.4	3.2	0.4	4.4
W	ppm	4	5.5	5.5	9	4	9	4.5	7.5	4	6.5	2.5	5	4	5

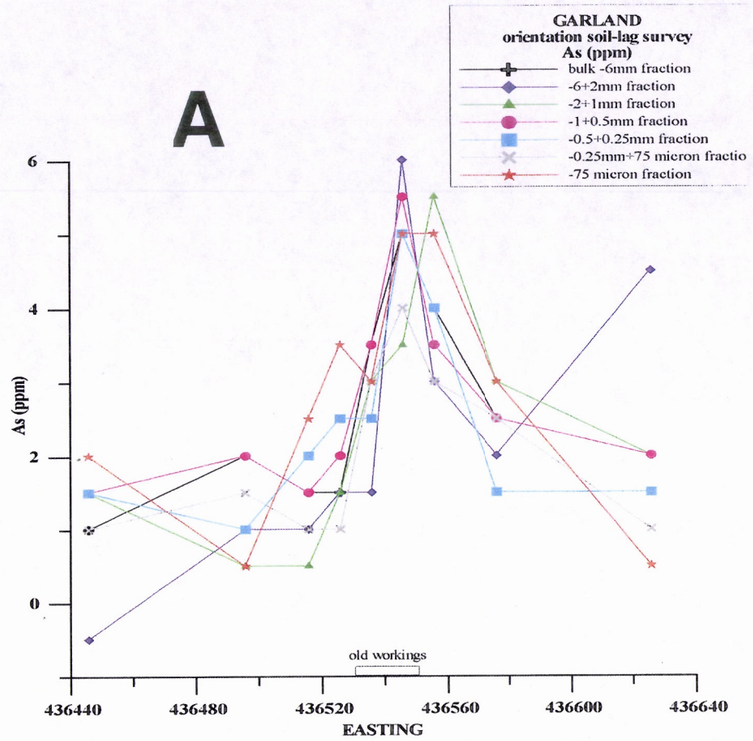
A
GARLAND
orientation soil-lag survey
As (ppm)
bulk -6mm fraction
-6+2mm fraction
-2+1mm fraction
-1+0.5mm fraction
-0.5+0.25mm fraction
-0.25mm+75 micron fractio
-75 micron fraction
As (ppm)
0
2
4
6
old workings
436440
436480
436520
436560
436600
436640
EASTING

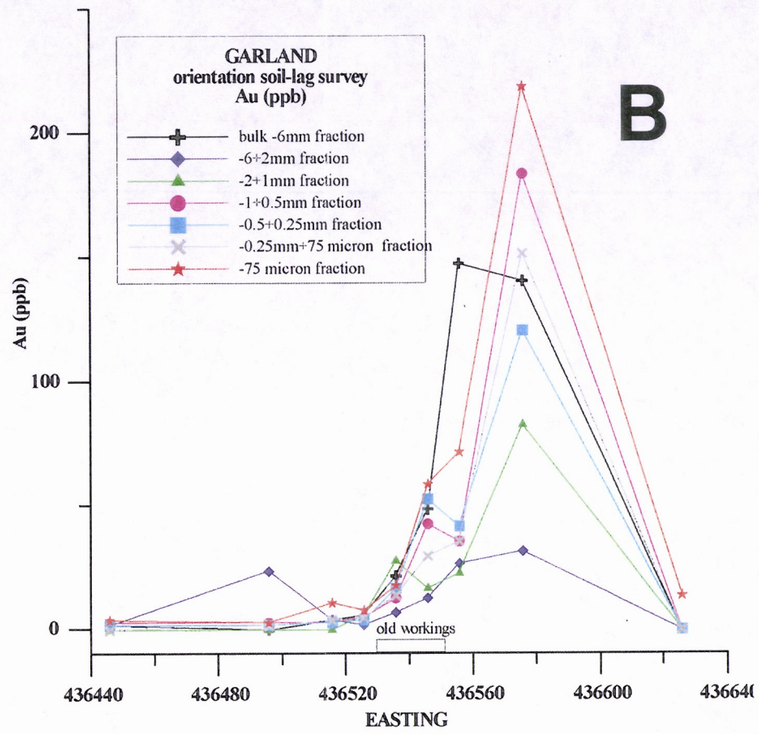
B
GARLAND
orientation soil-lag survey
Au (ppb)
bulk -6mm fraction
-6+2mm fraction
-2+1mm fraction
-1+0.5mm fraction
-0.5+0.25mm fraction
-0.25mm+75 micron fraction
-75 micron fraction
Au (ppb)
0
100
200
old workings
436440
436480
436520
436560
436600
436640
EASTING

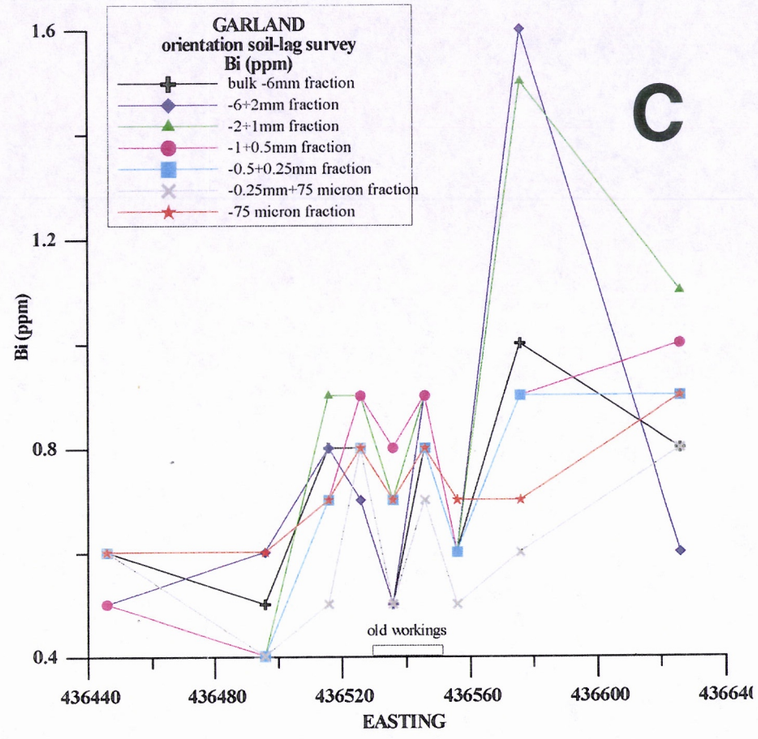
C
GARLAND
orientation soil-lag survey
Bi (ppm)
bulk -6mm fraction
-6+2mm fraction
-2+1mm fraction
-1+0.5mm fraction
-0.5+0.25mm fraction
-0.25mm+75 micron fraction
-75 micron fraction
Bi (ppm)
0.4
0.8
1.2
1.6
old workings
436440
436480
436520
436560
436600
436640
EASTING

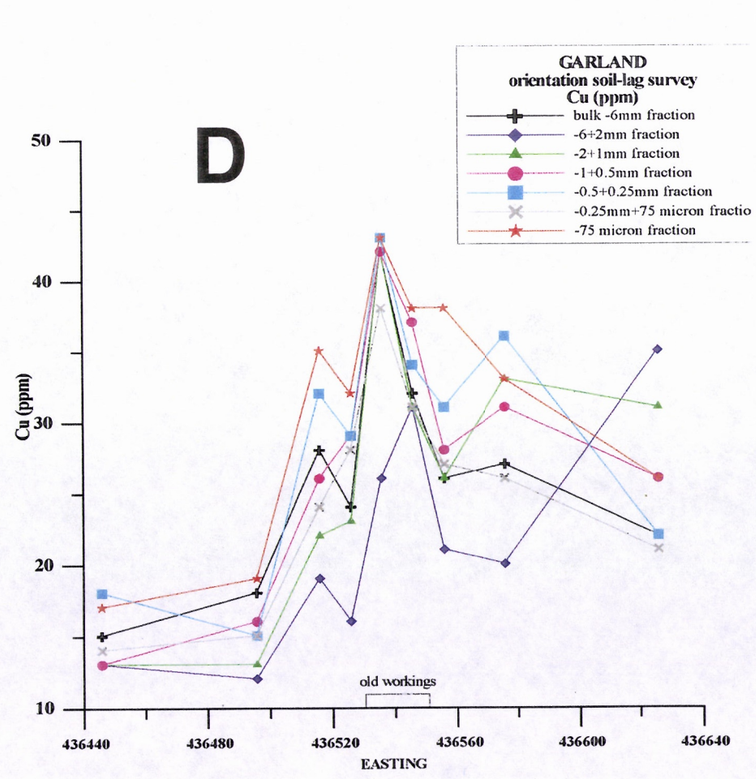
D
GARLAND
orientation soil-lag survey
Cu (ppm)
bulk -6mm fraction
-6+2mm fraction
-2+1mm fraction
-1+0.5mm fraction
-0.5+0.25mm fraction
-0.25mm+75 micron fractio
-75 micron fraction
Cu (ppm)
10
20
30
40
50
old workings
436440
436480
436520
436560
436600
436640
EASTING

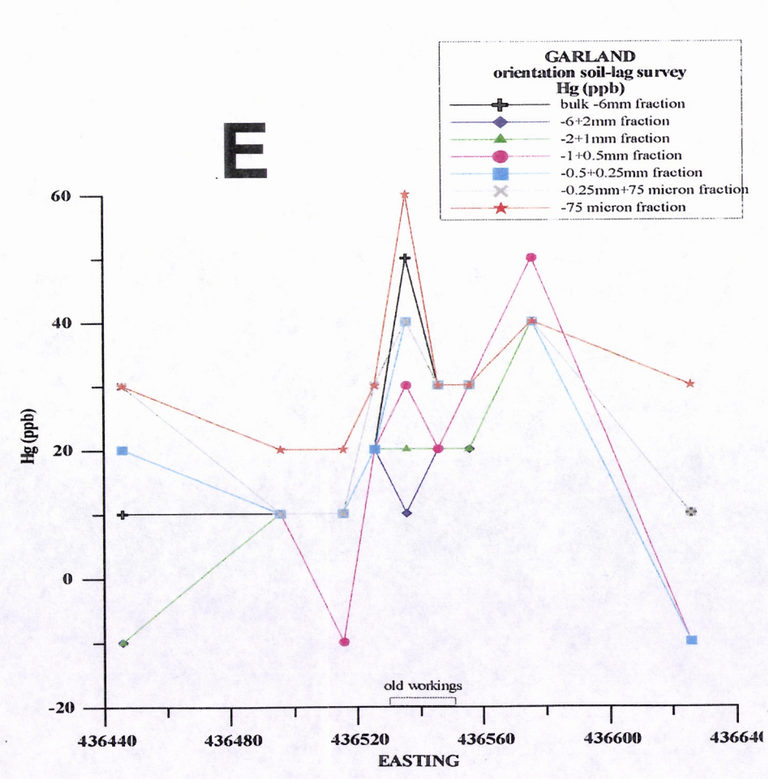
E
GARLAND
orientation soil-lag survey
Hg (ppb)
bulk -6mm fraction
-6+2mm fraction
-2+1mm fraction
-1+0.5mm fraction
-0.5+0.25mm fraction
-0.25mm+75 micron fraction
-75 micron fraction
Hg (ppb)
-20
0
20
40
60
old workings
436440
436480
436520
436560
436600
436640
EASTING

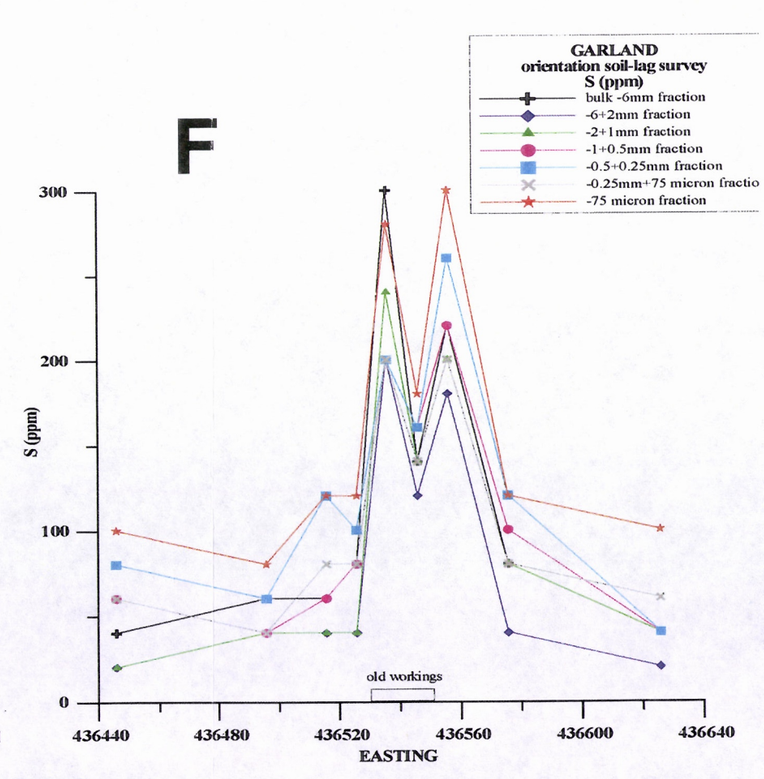
F
GARLAND
orientation soil-lag survey
S (ppm)
bulk -6mm fraction
-6+2mm fraction
-2+1mm fraction
-1+0.5mm fraction
-0.5+0.25mm fraction
-0.25mm+75 micron fractio
-75 micron fraction
S (ppm)
0
100
200
300
old workings
436440
436480
436520
436560
436600
436640
EASTING

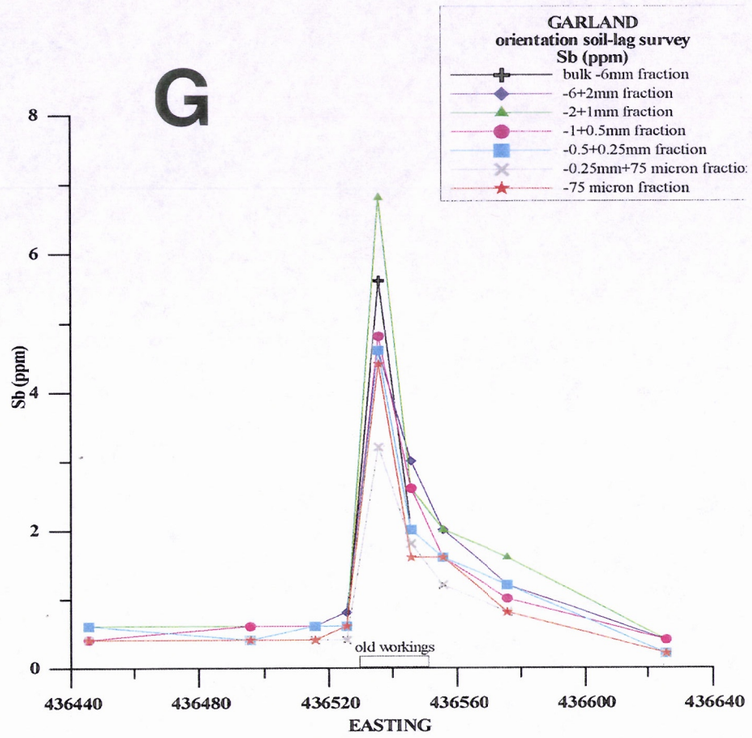
G
GARLAND
orientation soil-lag survey
Sb (ppm)
bulk -6mm fraction
-6+2mm fraction
-2+1mm fraction
-1+0.5mm fraction
-0.5+0.25mm fraction
-0.25mm+75 micron fractio
-75 micron fraction
Sb (ppm)
0
2
4
6
8
436440
436480
436520
436560
436600
436640
EASTING
old workings

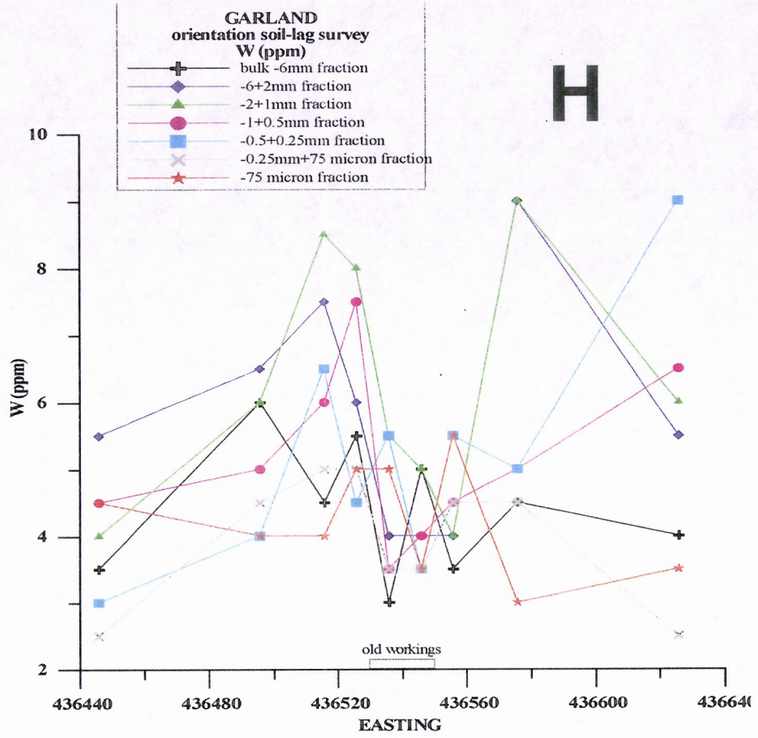
H
GARLAND
orientation soil-lag survey
W (ppm)
bulk -6mm fraction
-6+2mm fraction
-2+1mm fraction
-1+0.5mm fraction
-0.5+0.25mm fraction
-0.25mm+75 micron fraction
-75 micron fraction
W (ppm)
2
4
6
8
10
436440
436480
436520
436560
436600
436640
EASTING
old workings

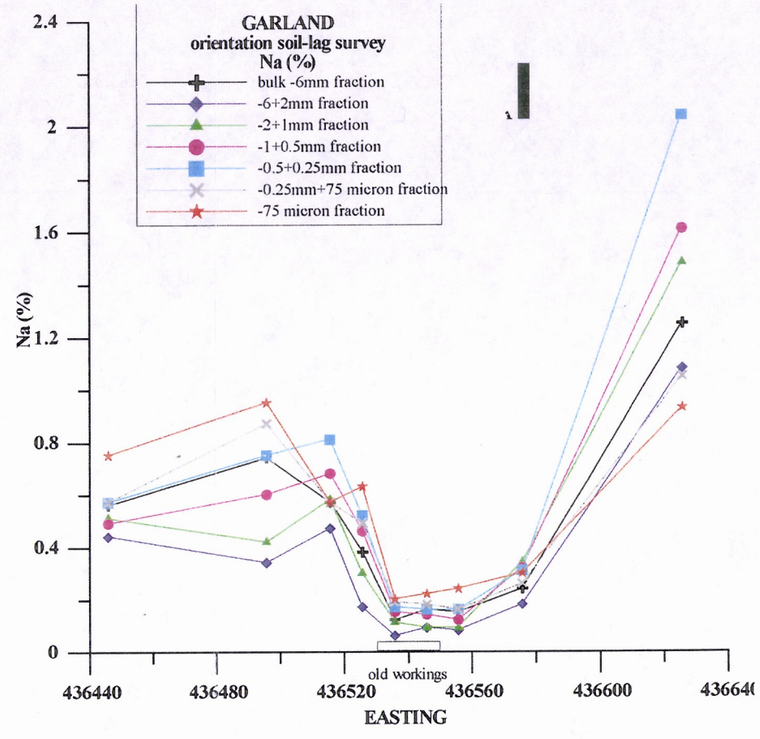
I
GARLAND
orientation soil-lag survey
Na (%)
bulk -6mm fraction
-6+2mm fraction
-2+1mm fraction
-1+0.5mm fraction
-0.5+0.25mm fraction
-0.25mm+75 micron fraction
-75 micron fraction
Na (%)
0
0.4
0.8
1.2
1.6
2
2.4
436440
436480
436520
436560
436600
436640
EASTING
old workings

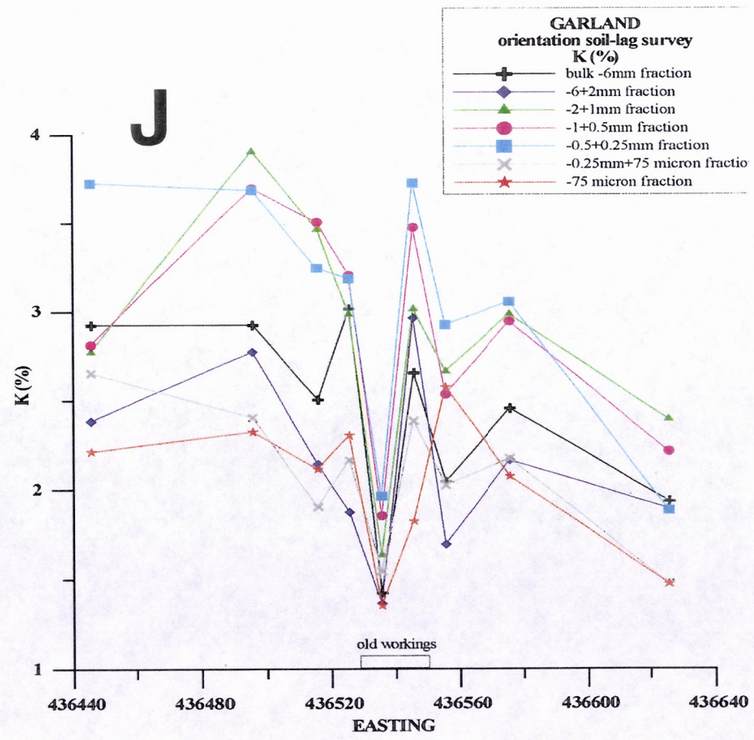
J
GARLAND
orientation soil-lag survey
K (%)
bulk -6mm fraction
-6+2mm fraction
-2+1mm fraction
-1+0.5mm fraction
-0.5+0.25mm fraction
-0.25mm+75 micron fractio
-75 micron fraction
K (%)
1
2
3
4
436440
436480
436520
436560
436600
436640
EASTING
old workings

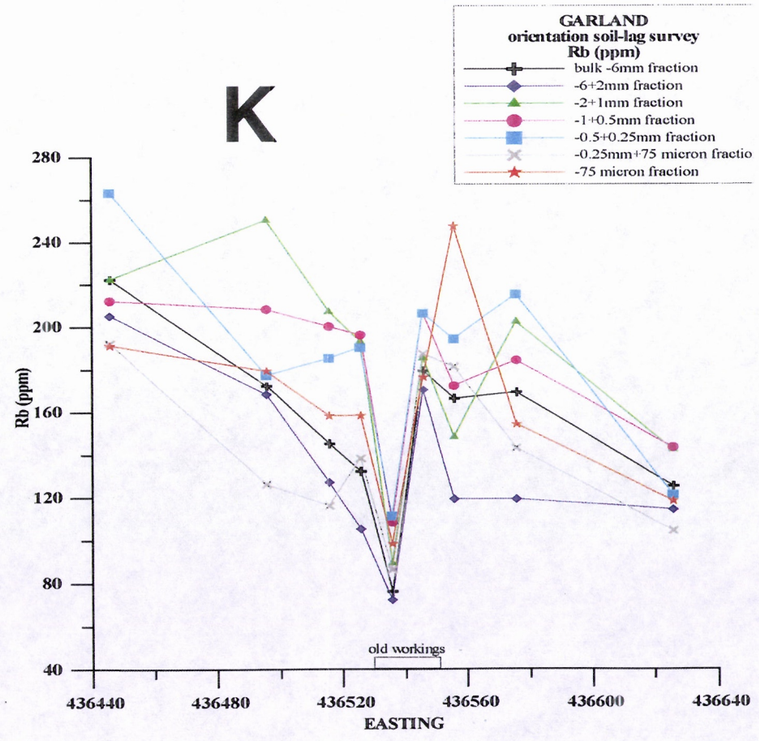
K
GARLAND
orientation soil-lag survey
Rb (ppm)
bulk -6mm fraction
-6+2mm fraction
-2+1mm fraction
-1+0.5mm fraction
-0.5+0.25mm fraction
-0.25mm+75 micron fractio
-75 micron fraction
Rb (ppm)
40
80
120
160
200
240
280
436440
436480
436520
436560
436600
436640
EASTING
old workings

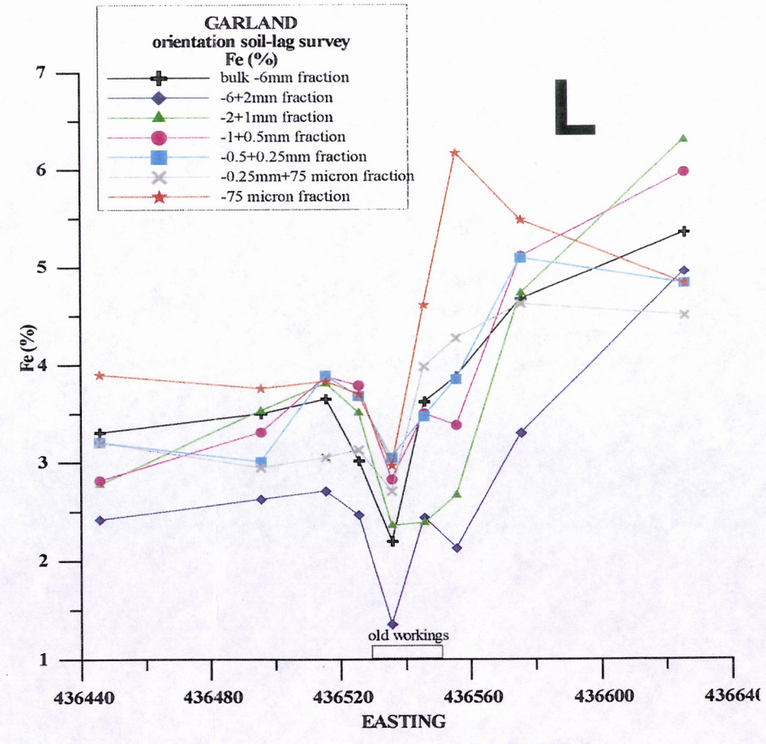
L
GARLAND
orientation soil-lag survey
Fe (%)
bulk -6mm fraction
-6+2mm fraction
-2+1mm fraction
-1+0.5mm fraction
-0.5+0.25mm fraction
-0.25mm+75 micron fraction
-75 micron fraction
Fe (%)
1
2
3
4
5
6
7
436440
436480
436520
436560
436600
436640
EASTING
old workings

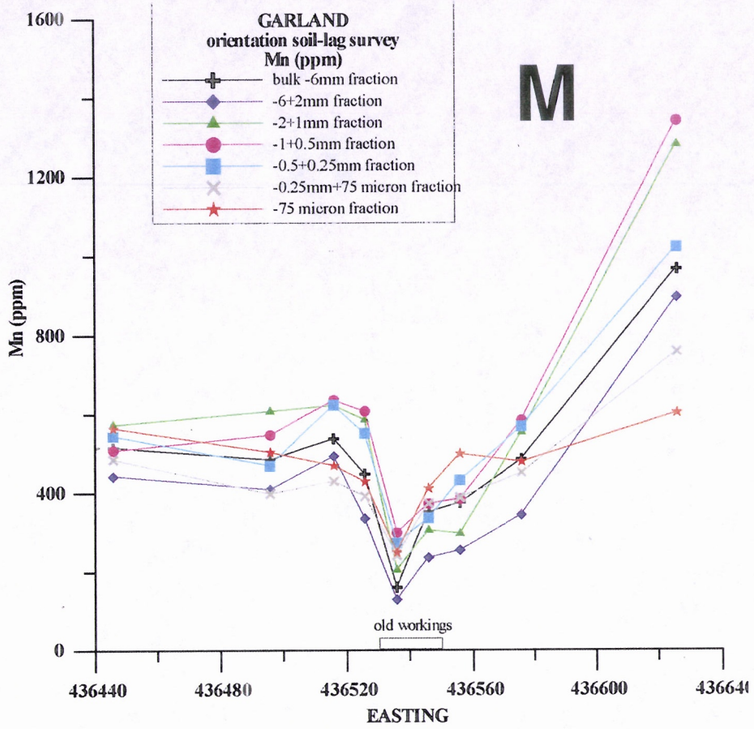
M
GARLAND
orientation soil-lag survey
Mn (ppm)
bulk -6mm fraction
-6+2mm fraction
-2+1mm fraction
-1+0.5mm fraction
-0.5+0.25mm fraction
-0.25mm+75 micron fraction
-75 micron fraction
Mn (ppm)
1600
1200
800
400
0
old workings
436440
436480
436520
436560
436600
436640
EASTING

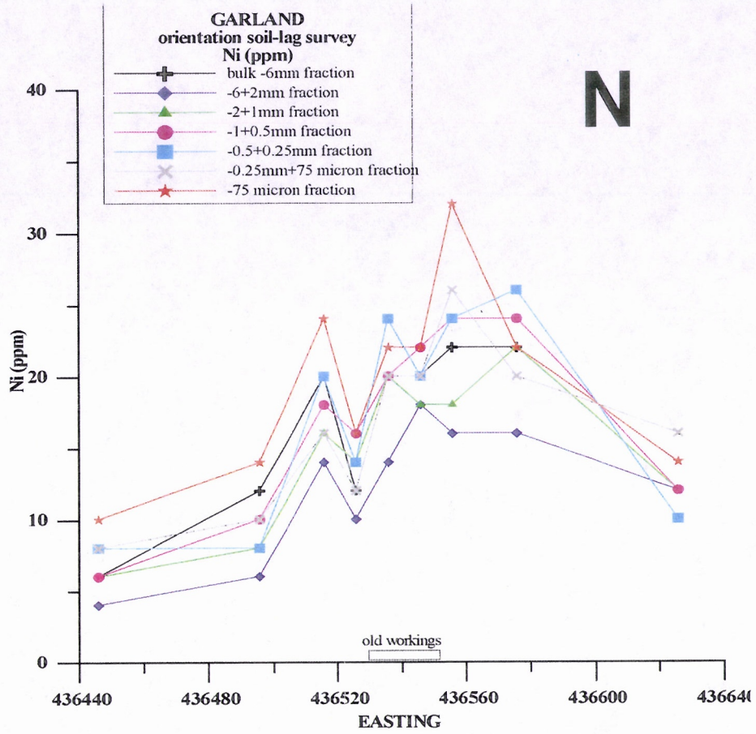
N
GARLAND
orientation soil-lag survey
Ni (ppm)
bulk -6mm fraction
-6+2mm fraction
-2+1mm fraction
-1+0.5mm fraction
-0.5+0.25mm fraction
-0.25mm+75 micron fraction
-75 micron fraction
Ni (ppm)
40
30
20
10
0
old workings
436440
436480
436520
436560
436600
436640
EASTING

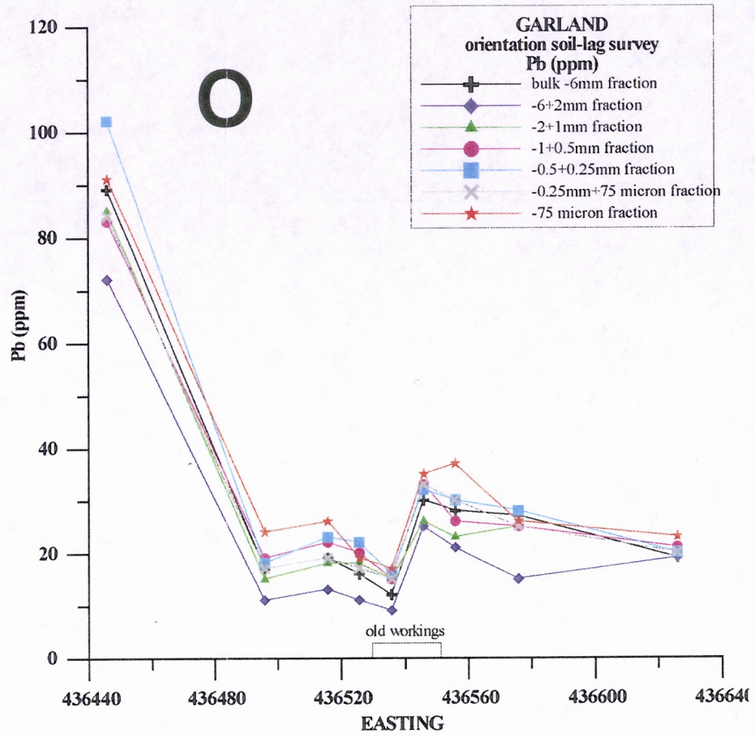
O
GARLAND
orientation soil-lag survey
Pb (ppm)
bulk -6mm fraction
-6+2mm fraction
-2+1mm fraction
-1+0.5mm fraction
-0.5+0.25mm fraction
-0.25mm+75 micron fraction
-75 micron fraction
Pb (ppm)
120
100
80
60
40
20
0
old workings
436440
436480
436520
436560
436600
436640
EASTING

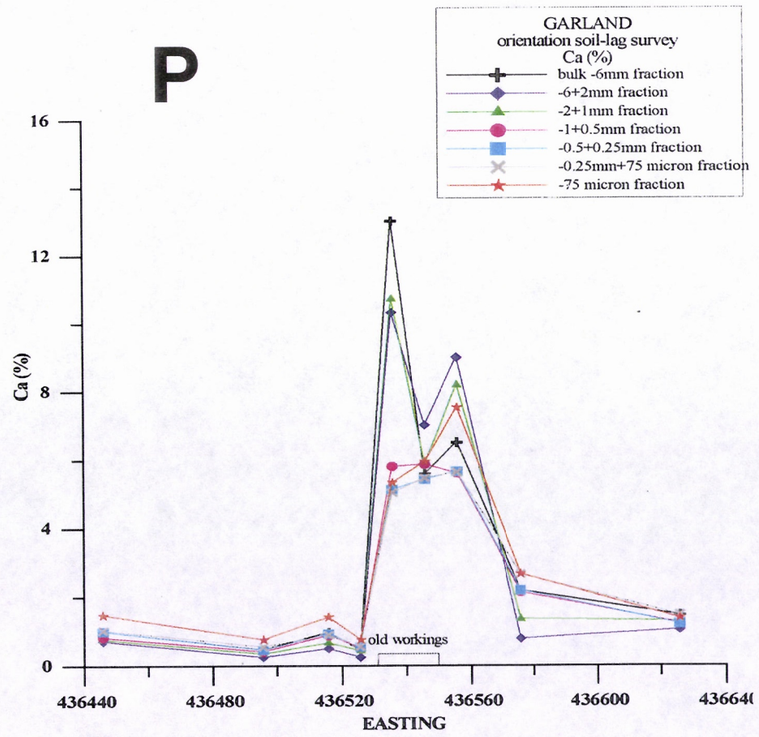
P
GARLAND
orientation soil-lag survey
Ca (%)
bulk -6mm fraction
-6+2mm fraction
-2+1mm fraction
-1+0.5mm fraction
-0.5+0.25mm fraction
-0.25mm+75 micron fraction
-75 micron fraction
Ca (%)
16
12
8
4
0
old workings
436440
436480
436520
436560
436600
436640
EASTING

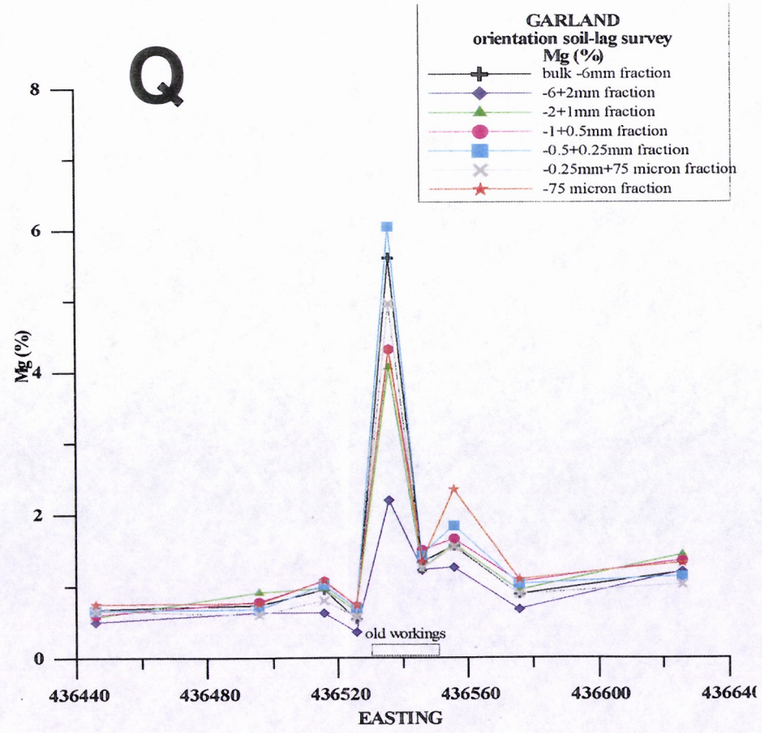
Q
GARLAND
orientation soil-lag survey
Mg (%)
bulk -6mm fraction
-6+2mm fraction
-2+1mm fraction
-1+0.5mm fraction
-0.5+0.25mm fraction
-0.25mm+75 micron fraction
-75 micron fraction
Mg (%)
8
6
4
2
0
old workings
436440
436480
436520
436560
436600
436640
EASTING

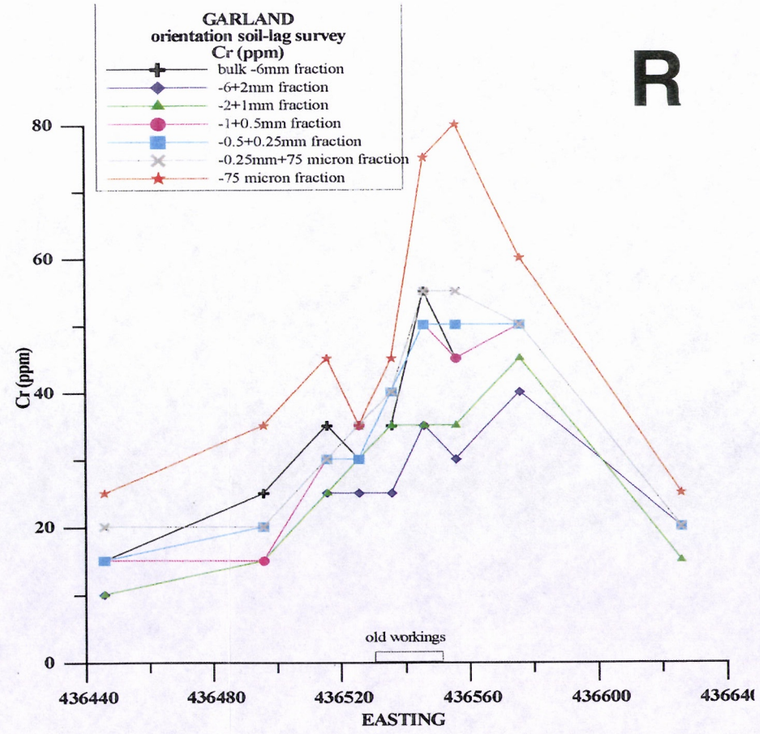
R
GARLAND
orientation soil-lag survey
Cr (ppm)
bulk -6mm fraction
-6+2mm fraction
-2+1mm fraction
-1+0.5mm fraction
-0.5+0.25mm fraction
-0.25mm+75 micron fraction
-75 micron fraction
Cr (ppm)
80
60
40
20
0
old workings
436440
436480
436520
436560
436600
436640
EASTING

S

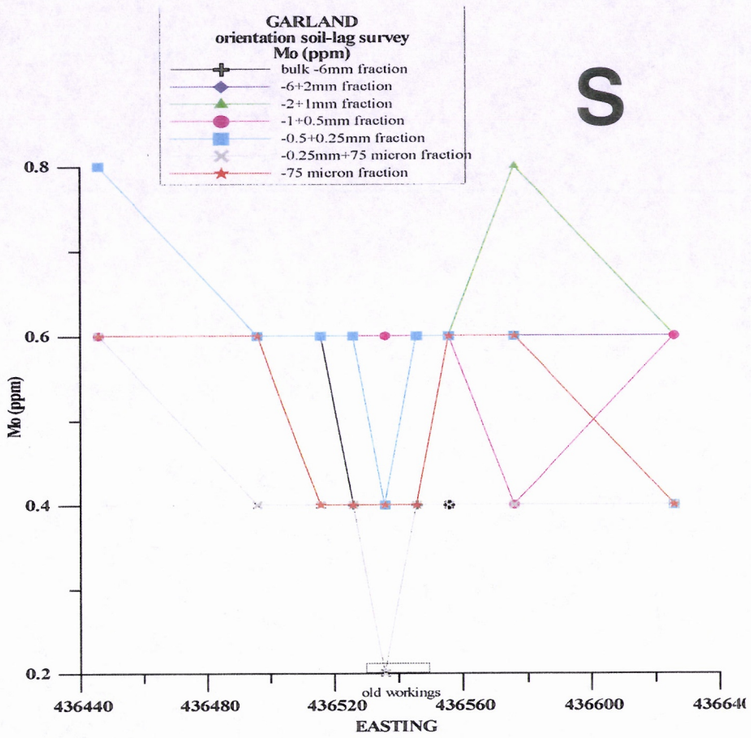
GARLAND
orientation soil-lag survey
Mo (ppm)
bulk -6mm fraction
-6+2mm fraction
-2+1mm fraction
-1+0.5mm fraction
-0.5+0.25mm fraction
-0.25mm+75 micron fraction
-75 micron fraction
Mo (ppm)
0.8
0.6
0.4
0.2
old workings
436440
436480
436520
436560
436600
EASTING

T

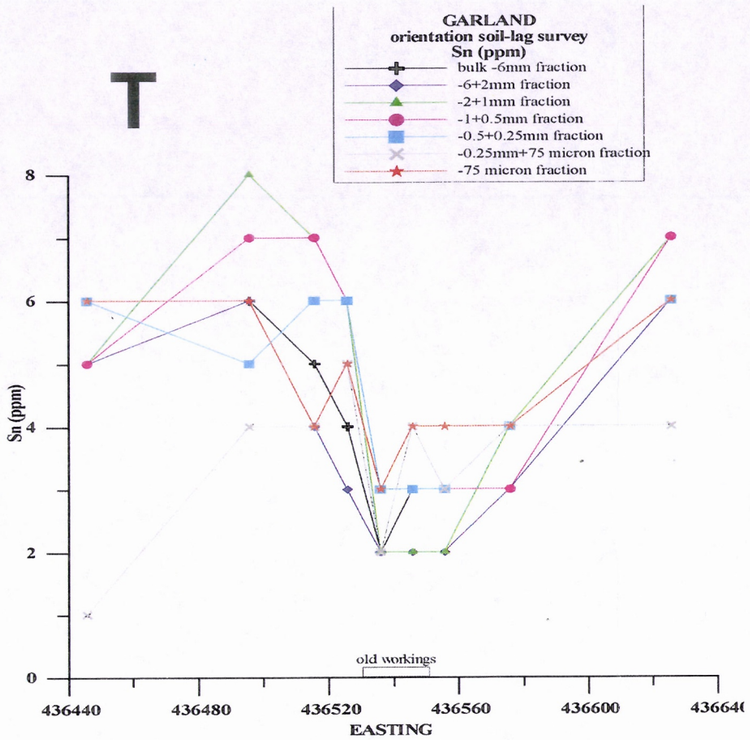
GARLAND
orientation soil-lag survey
Sn (ppm)
bulk -6mm fraction
-6+2mm fraction
-2+1mm fraction
-1+0.5mm fraction
-0.5+0.25mm fraction
-0.25mm+75 micron fraction
-75 micron fraction
Sn (ppm)
8
6
4
2
0
old workings
436440
436480
436520
436560
436600
EASTING

U

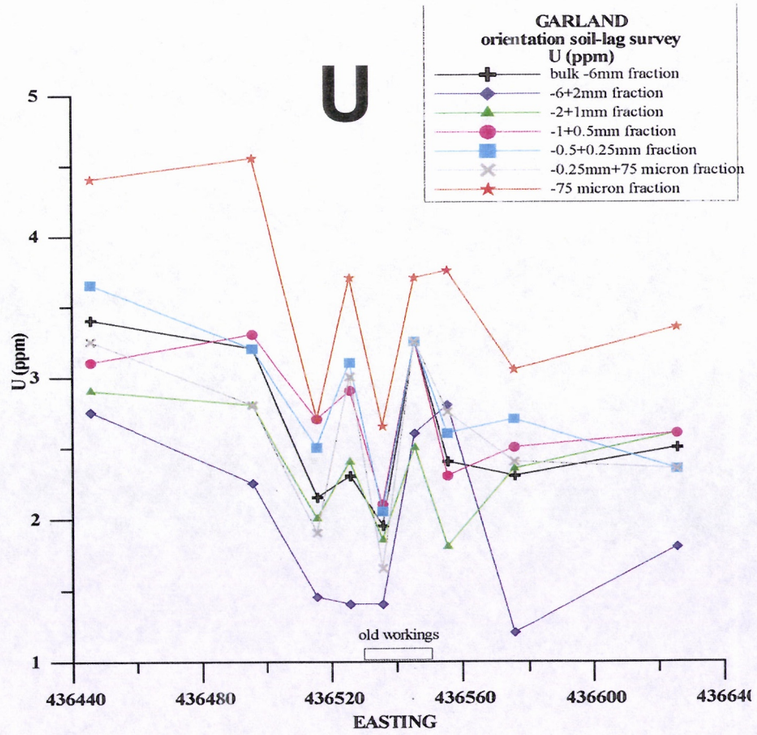
GARLAND
orientation soil-lag survey
U (ppm)
bulk -6mm fraction
-6+2mm fraction
-2+1mm fraction
-1+0.5mm fraction
-0.5+0.25mm fraction
-0.25mm+75 micron fraction
-75 micron fraction
U (ppm)
5
4
3
2
1
old workings
436440
436480
436520
436560
436600
EASTING

V

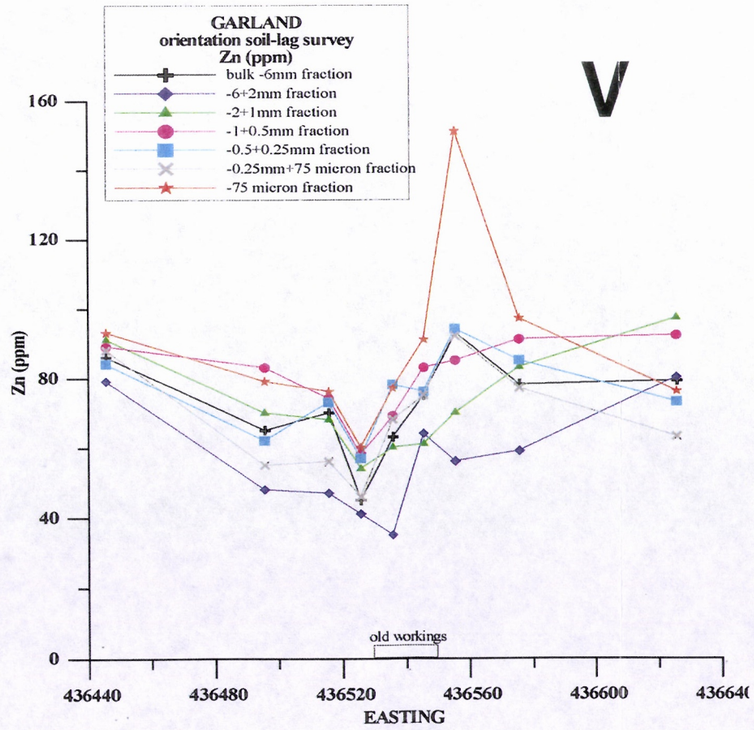
GARLAND
orientation soil-lag survey
Zn (ppm)
bulk -6mm fraction
-6+2mm fraction
-2+1mm fraction
-1+0.5mm fraction
-0.5+0.25mm fraction
-0.25mm+75 micron fraction
-75 micron fraction
Zn (ppm)
160
120
80
40
0
old workings
436440
436480
436520
436560
436600
EASTING

7.3 Geochemistry

7.3.1 Elements associated with mineralisation (As, Au, Bi, Cu, Hg, S, Sb, W)

Arsenic

There is a low-level peak along strike from the old workings, with maxima of 4-6 ppm over a background of 1-2 ppm. Concentrations are similar for each size fraction (Figure 6A).

Gold

There is a significant peak in Au concentrations about 35 m east of the old workings (Figure 6B), although there are above-background concentrations in most fractions (particularly in the bulk <6 mm) along strike from the old workings. Concentrations generally increase from the coarsest (31 ppb; 6-2 mm) to the finest fraction (218 ppb; <75 μm). Backgrounds are generally at or below the detection limit (1 ppb). The peak to the east of the old workings may indicate a previously unrecognised zone of mineralisation.

Bismuth

The distribution of Bi is very erratic but, like Au, has a prominent peak to the east of the old workings (Figure 6C). Bismuth concentrations are generally greatest in the coarse fractions (6-2 mm and 2-1 mm). Backgrounds are at 0.6 ppm or less, with 0.7-0.9 ppm along strike from the old workings, and 1.5-1.6 ppm (in the coarse fractions) to the east.

Copper

An ill-defined Cu peak occurs along strike from the old workings (Figure 6D) and may indicate minor Cu associated with the mineralisation (Hossfeld, 1940). Concentrations are generally greater in the finer fractions. Backgrounds are less than 20 ppm in the west, but increase to 20-35 ppm east of the old workings, and may reflect more mafic biotitic schists in the east. Peak concentrations vary from 30-45 ppm (from coarse to fine fractions).

Mercury

The distribution of Hg is shown in Figure 6E. Two peaks occur: along strike from the old workings, and about 35 m to the east (coinciding with the Au peak). Mercury concentrations appear to be generally greater in the finer fractions. Backgrounds appear to be 30 ppb or less, with peaks up to 60 ppb. The analytical method used in this study (aqua regia digest; 10 ppb detection limit) is not the most precise; a better analytical technique may provide clearer trends.

Sulfur

Sulfur shows a double peak over the lode and also 20 m to the east (Figure 6F) similar to Ca and Mg. The S possibly occurs as gypsum and may reflect pyrite at depth. Highest S concentrations tend to be in the fine fractions. Peak concentrations vary from 200-300 ppm over a background below 100 ppm.

Antimony

Antimony peaks over the strike extension of the lode (Figure 6G), with a gradual tailing off to the east. Concentrations are generally greatest in the intermediate and fine fractions. Backgrounds are <1 ppm, with peaks at 3-7 ppm.

Tungsten

Tungsten concentrations are erratic and show little systematic variation along the traverse, apart from a general decrease along strike from the old workings (Figure 6H), although there may be subtle peaks along the margins of the lode in some of the coarser fractions. The peaks in the coarse fractions (6-2 mm and 2-1 mm) east of the old workings appear to coincide with the Au peak. Concentrations tend to be greatest in the coarse fractions. Peaks and backgrounds are somewhat variable (see Table 1).

7.3.2 Lithology-associated elements (Na, K, Rb, Fe, Mn, Ni, Pb, Rb)

Sodium

Sodium decreases over the strike extension of the old workings (Figure 6I) due to calcrete and/or silicification from the lode. To the west, concentrations are generally consistent (0.4-0.8%), but increase sharply at the eastern end of the traverse (presumably related to abundant feldspar in the schists). Concentrations are greater in the fine than in the coarse fractions, except to the east of the old workings, where concentrations are greatest in the intermediate fractions. The influence of lithology and the presence of calcrete preclude the meaningful determination of peak and background abundances.

Potassium

Potassium decreases from west to east (due to the lithological factors outlined above; Figure 6J) and shows a marked decrease along strike from the old workings (due to silicification and/or calcrete abundance). Potassium concentrations are generally greatest in the intermediate fractions (2-1 mm, 1-0.5 mm, and 0.5-0.25 mm) and reflect the grain size of K-bearing minerals in the samples. Because of the lithological controls on K distribution, it is not possible to determine peak and background concentrations.

Rubidium

Rubidium is more abundant to the west of the old workings (Figure 6K) and shows a marked decrease over the strike extension of the old workings (due to calcrete and/or silicification) similarly to K (Figure 6J). In some of the finer fractions there are small peaks along the margins of the lode – this may reflect Rb in an alteration halo. The intermediate fractions (2-1 mm, 1-0.5 mm, and 0.5-0.25 mm) generally have the greatest Rb concentrations (as for K).

Iron

Iron concentrations increase from west to east (Figure 6L), probably reflecting differences in composition between the more felsic schists to the west and the more mafic schists in the east. Iron also shows a marked decrease along strike from the old workings, presumably indicating the silicification along the lode and/or abundance of calcrete. Iron concentrations are generally greater in the fine than in the coarse fractions. To the west of the old workings, Fe concentrations are relatively constant within each fraction (2.5 % in the coarsest fraction to about 3.8 % in the finest), but to the east, concentrations are typically over 4% Fe. Because of the apparent lithological control on the distribution of Fe, it is not possible to determine peak and background concentrations.

Manganese

Manganese concentrations increase from west to east along the traverse (Figure 6M), apart from a distinct decrease over the strike extension of the old workings (due to silicification and/or calcrete). Manganese concentrations appear to be greatest in the intermediate fractions (2-1 mm, 1-0.5 mm, and 0.5-0.25 mm). It is not possible to determine meaningful peak and background concentrations for Mn because of lithological factors and dilution by calcrete.

Nickel

Nickel concentrations increase slightly from west to east (Figure 6N) with a subtle peak to the east of the old workings (similar to Cr and Fe). Nickel concentrations do not appear significantly affected either by calcrete or silicification. Concentrations are generally greater in the finer than in the coarser fractions.

Lead

Lead shows a minor decrease over the strike extension of the old workings (Figure 6O) due to calcrete and/or silicification, with slightly greater concentrations to the east than to the west (presumably reflecting lithology), except for the westernmost sample. The reasons for this significantly greater concentration are unclear, although contamination is possible. Lead tends to be greatest in the finer fractions. There does not appear to be any Pb associated with the lode (and mineralisation). It is not

possible to determine meaningful background and peak abundances, due to lithological variation and the lack of Pb in the lode.

7.3.3 Regolith-associated elements (Ca, Mg)

Calcium

The distribution of Ca is shown in Figure 6P. A broad peak occurs along strike from the old workings and for about 20 m to the east (corresponding to the zone of most abundant calcrete). In the zone of peak concentrations, Ca is most abundant in the coarse fractions; the reverse is true in the flanking zones. Because of the calcrete, it is not possible to determine meaningful peak and background concentrations.

Magnesium

Magnesium shows a subtle increase from west to east, due to lithology; (Figure 6Q), but there is a distinct peak along strike from the old workings. This peak is probably related to dolomite and/or magnesian calcite in the calcrete, rather than hydrothermal alteration of the lode. Magnesium concentrations are similar for each size fraction, except for the 6-2 mm fraction, in which concentrations are distinctly less. It is not possible to determine meaningful peak and backgrounds for Mg, because of lithological considerations and the influence of calcrete.

There is no consistent relationship between Ca and Au in any of the soil or lag fractions, indicating that the regolith carbonates are probably not pedogenic (Figure 7) and that calcrete sampling may be inappropriate for Au search in this region.

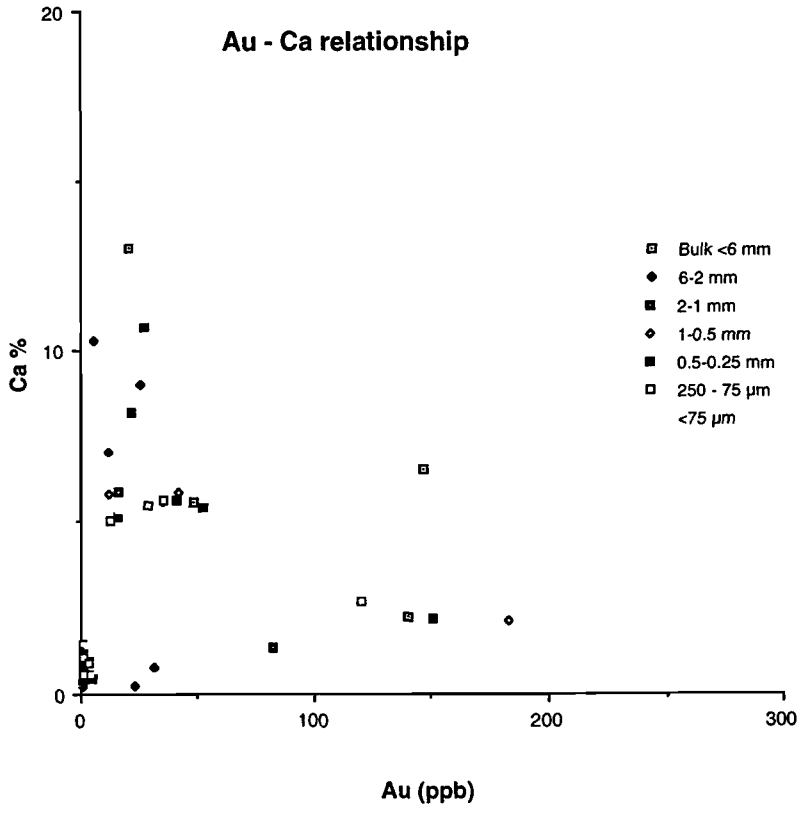

Figure 7. Scatterplot of Au and Ca for all soil and lag fractions.

7.3.4 Elements lacking a systematic distribution (Ag, Cr, Mo, Se, Sn, Te, U, Zn)

Silver
For every size fraction for every sample, Ag concentrations (not plotted) are below the lower limit of detection (0.5 ppm).

Chromium
Chromium concentrations (Figure 6R) are greatest at about 10-20 m east of the old workings (Figure 2); the reason for this is uncertain. Concentrations are greater in the fine than in the coarse fractions. Backgrounds are around 10-20 ppm; peak values range from 30 ppm in the coarse fractions to 80 ppm in the finest (<75 μm) fraction.

Molybdenum
Molybdenum shows no clear trends, apart from an apparent decrease along strike from the old workings (Figure 6S).

Selenium
Selenium concentrations (not plotted) are less than 2 ppm for all fractions for all sample sites and show no systematic variation.

Tin
Tin shows a decrease along strike from the old workings (Figure 6T) due to calcrete abundance and/or silicification. Concentrations are greatest in the intermediate fractions.

Tellurium
All Te concentrations (not plotted) are below the lower limit of detection (0.2 ppm).

Uranium
Uranium concentrations show no meaningful variation across the traverse (Figure 6U), apart from a decrease over the lode. There is no correlation between U and calcrete. Concentrations are greatest in the finer fractions, particularly <75 μm.

Zinc
Zinc shows no systematic variation, apart from a decrease over the lode (Figure 6V). Concentrations are greatest in the fine fractions.

8. CONCLUSIONS

Soil and lag over the strike extension of the mineralised zone are characterised by elevated concentrations of As, Au, Bi, Cu, Hg, S, Sb, and W. Their abundances are independent of soil/lag type and are not diluted by calcrete. Bismuth and W show the best response (contrast and abundance) in the coarsest fraction (6-2 mm), whereas Cu, Hg, S and Sb are most abundant in the finest fraction (<75 μm). Gold is most abundant in the <75 μm fraction, but also shows some response in the 6-2 mm fraction. Elevated Rb and W at the margins of the lode may indicate hydrothermal alteration. The other elements (Cr, Cu, Fe, K, Mn, Na, Ni, Pb, Sn, U, and Zn) are depleted along strike from the old workings, by dilution due to calcrete and/or silicification.

Except for Bi and W, concentrations tend to be greatest in the finest fractions and K, Mn, Na, Rb, Sb and Sn are most abundant in the intermediate fractions. The generally greater concentrations in the intermediate and fine fractions (particularly <75 μm) would indicate that these fractions are the best sampling medium. Ideally, both the 6-2 mm and <75 μm fractions should be collected and analysed for the appropriate elements. A compromise would be the <2 mm fraction, which would simplify sample collection and preparation. Sampling of coarse lag (6-2 mm) only is likely to detect Au mineralisation, but anomalies may be subtle and/or irregular for Bi and W.

The partitioning of the elements associated with mineralisation into two general size fractions is not fully understood and requires further study. The concentration of Au, Bi and W into the coarse fractions (i.e., coarse lag) implies that these elements possibly are distributed heterogeneously throughout the siliceous lode and that their abundance is dependent on the collection of relatively coarse lag. The association of the other elements with the fine fractions indicates that their occurrence may be dependent upon the occurrence of a particular phase (e.g., Fe oxides) which is relatively minor in the lode and which is either preferentially weathered out into the finer soil fractions or forms secondary coatings on relatively fine fragments of lode. At this stage it is not clear whether there is any geochemical difference (in trace element concentrations) between ferruginous silcrete and siliceous lode.

From the data above, the general conclusions for mineral exploration in the Winnecke area are:

(i) the element suite associated with mineralisation is As, Au, Bi, Cu, Hg, S, Sb and W;
(ii) the geochemical signature of soil and lag are dependent on size fraction;
(iii) the width of the mineralised zones appears to be narrow, the anomalies are narrow and therefore adequate sample spacing is critical; at Garland, the sample spacing should not exceed 25 m; if wider sample spacing is desirable, a triangular, rather than a square, grid should be employed;
(iv) an adequate geological and regolith map is required prior to any detailed soil-lag sampling programmes;
(v) sampling of calcretes is likely to be inappropriate for Au search here.

Further studies need to be conducted at other mineralised localities (e.g., Junction, Coorong, Big Gun, Coronation) in the Winnecke area to determine the applicability of the general conclusions above. This should be in conjunction with petrological and mineralogical studies of the materials sampled.

9. ACKNOWLEDGEMENTS

Sample sieving was by P. Thornley and milling was by J.F. Crabb. Li Shu provided detailed regolith-landform mapping (Figure 5) from the ARGOS Project, which has been released from confidentiality by the N.T. Geological Survey (July, 2000). T. Naughton prepared colour artwork. I.D.M. Robertson, and C.R.M. Butt provided critical review of the manuscript. All this assistance is acknowledged with appreciation.

10. REFERENCES

Clarke, D., 1971 Winnecke – Authority to Prospect 1721, Northern Territory. Progress report. [Northern Territory Geological Survey company report CR95/650]

Forman, D.J., 1971 The Arltunga Nappe Complex, MacDonnell Ranges, Northern Territory, Australia. Journal of the Geological Society of Australia 18: 173-182.

Hossfeld, P.S., 1940 The Winnecke Goldfield, eastern MacDonnell Ranges district. Aerial, Geological and Geophysical Survey of Northern Australia, Northern Territory, Report 40.

Joklik, G.F., 1955 The geology and mica-fields of the Harts Range, central Australia. Bureau of Mineral Resources, Australia, Bulletin 26.

Robertson, I.D.M., Dyson, M., Hudson, E.G., Crabb, J.F., Willing, M.J., and Hart, M.K.W., 1996 A case-hardened, low contamination ring mill for multi-element geochemistry. Journal of Geochemical Exploration 57: 153-158.

Shaw, R.D. and Langworthy, A.P., 1984 Strangways Range region, Northern Territory. 1:100 000 geological map commentary. Bureau of Mineral Resources, Australia.

Skwarnecki, M., Li Shu, Fraser S.J. and Robertson, I.D.M. 2000. Geochemical orientation surveys and regolith geology in the S.W. Arunta Province, Northern Territory (ARGOS Project). CRC LEME Restricted Report 129R.

Wygralak, A.S., 1995 Alice Springs SF53-14, 1:250 000 mineral deposit data series. Northern Territory Geological Survey.

Wygralak, A.S. and Bajwah, Z.U., 1998 Geology and mineralisation of the Arunta Inlier, Northern Territory. AGSO Journal of Australian Geology and Geophysics 17(3): 35-45.

APPENDIX 1

DESCRIPTION OF SAMPLE SITES

APPENDIX 1 - Description of soil sample sites

Sample No	Easting	Northing	soil pH	Sample description
GA1	436536	7419189	9.5-10	Grey-brown calcareous soil with calcrete; quartz, calcrete, and lode-derived (silicified) lag
GA2	436526	7419189	7	Greyish orange-brown soil with abundant lode-derived (silicified and quartz-veined) lag; close to outcrop of lode
GA3	436516	7419189	7	Greyish orange-brown soil; lode-derived (silicified) and quartz lag; lesser amounts of hematitic silcrete lag
GA4	436496	7419189	6	Greyish orange-brown soil; lode-derived (silicified), quartz and hematitic silcrete lag; near outcrop of quartz-biotite-feldspar schist
GA5	436446	7419189	6	Greyish orange-brown soil on iron-oxide-stained outcrop of biotite-muscovite-quartz-feldspar schist; rare quartz lag
GA6	436546	7419189	9.5-10	Grey-brown calcareous soil with calcrete; quartz, calcrete, hematitic silcrete and lode-derived (silicified) lag
GA7	436556	7419189	9.5-10	Grey-brown calcareous soil with calcrete; calcrete, hematitic silcrete and lode-derived (silicified) lag; minor quartz lag
GA8	436576	7419189	9	Greyish orange-brown soil with some calcrete; quartz, hematitic silcrete and lode-derived (silicified) lag
GA9	436626	7419189	8	Greyish orange-brown soil; quartz and biotite-quartz-feldspar schist lag

APPENDIX 2

SAMPLE FRACTION WEIGHTS

APPENDIX 2 - Weights of size fractions (g)

Fraction\Sample No	GA1	GA2	GA3	GA4	GA5	GA6	GA7	GA8	GA9
<6 mm bulk	348.2	322.4	425.1	307.5	362.1	412.4	285.8	314.2	413
6-2 mm	282	286.4	356.8	317.8	263.4	250.6	258.1	334.6	414.4
2-1 mm	172.3	260.2	154.5	135.6	130.6	119.2	114.3	149.9	140.6
1-0.5 mm	127.1	448.5	315.1	297	331.2	248.5	184.4	417	222.5
0.5-0.25 mm	295.3	245.5	202.3	224.9	271.9	178.7	145	275.5	186.3
250 mm-75 µm	698.8	1017	1129.5	1131.3	1098.3	1136.1	1127.4	1022.8	1062.8
<75 µm	176.3	228.5	445.4	203	156.5	242.8	248.4	87.3	495.9
Sum of < 2mm fraction	1469.8	2199.7	2246.9	1991.8	1990.5	1925.3	1819.5	1952.5	2108.1

APPENDIX 3

TABULATED GEOCHEMISTRY

APPENDIX 3 - Tabulated Geochemistry

FieldNo	LabSeqNo	LibNo	Easting	Northing	Method Element Detection limit Fraction	ICP-MS Au(AR) 1 ppb	ICP-MS Hg(AR) 10 ppb	ICP-OES Cu 1 ppm	ICP-OES Fe 0.01 %	ICP-OES Mn 1 ppm	ICP-OES Mg 0.01 %	ICP-OES S 20 ppm	ICP-OES K 0.01 %	ICP-OES Na 0.01 %	ICP-OES Ca 0.01 %	ICP-OES Ni 2 ppm	ICP-OES Cr 5 ppm	ICP-OES Zn 1 ppm	ICP-MS Ag 0.5 ppm	ICP-MS As 0.5 ppm	ICP-MS Bi 0.1 ppm	ICP-MS Mo 0.2 ppm	ICP-MS Pb 1 ppm	ICP-MS Rb 0.02 ppm	ICP-MS Sb 0.2 ppm	ICP-MS Se 1 ppm	ICP-MS Sn 1 ppm	ICP-MS Te 0.2 ppm	ICP-MS U 0.05 ppm	ICP-MS W 0.5 ppm
GA1	L15-00150	L15-00101	436536	7419189	bulk <6 mm	21	50	42	2.19	158	5.6	300	1.42	0.12	13	20	35	63	-0.5	3.5	0.5	0.4	12	76	5.6	-1	2	-0.2	1.95	3
GA1	L15-00166	L15-00102	436536	7419189	6-2 mm	6	10	26	1.35	127	2.19	200	1.36	0.06	10.3	14	25	35	-0.5	1.5	0.5	0.4	9	71.6	4.6	1	2	-0.2	1.4	4
GA1	L15-00124	L15-00103	436536	7419189	2-1 mm	27	20	42	2.35	203	4.06	240	1.63	0.11	10.7	20	35	60	-0.5	3	0.7	0.4	15	89	6.8	1	2	-0.2	1.85	5.5
GA1	L15-00145	L15-00104	436536	7419189	1-0.5 mm	12	30	42	2.82	297	4.31	200	1.85	0.15	5.79	20	40	69	-0.5	3.5	0.8	0.6	15	108	4.8	-1	3	-0.2	2.1	3.5
GA1	L15-00123	L15-00105	436536	7419189	0.5-0.25 mm	16	40	43	3.04	271	6.04	200	1.96	0.17	5.11	24	40	78	-0.5	2.5	0.7	0.4	16	111	4.6	2	3	0.2	2.05	5.5
GA1	L15-00163	L15-00106	436536	7419189	0.25 mm-75mm	13	40	38	2.7	240	4.95	200	1.54	0.19	5.02	20	40	68	-0.5	3	0.5	0.2	15	85.5	3.2	1	2	-0.2	1.65	3.5
GA1	L15-00158	L15-00107	436536	7419189	<75 mm	17	60	43	2.96	247	4.31	280	1.35	0.2	5.32	22	45	77	-0.5	3	0.7	0.4	17	97.7	4.4	1	3	-0.2	2.65	5
GA2	L15-00161	L15-00108	436526	7419189	bulk <6 mm	5	20	24	3.01	446	0.53	80	2.31	0.38	0.44	12	30	45	-0.5	1.5	0.8	0.4	16	132	0.6	1	4	-0.2	2.3	5.5
GA2	L15-00153	L15-00109	436526	7419189	6-2 mm	1	20	16	2.46	333	0.35	40	1.87	0.17	0.23	10	25	41	-0.5	1.5	0.7	0.6	11	105	0.8	-1	3	-0.2	1.4	6
GA2	L15-00168	L15-00110	436526	7419189	2-1 mm	5	20	23	3.5	585	0.64	40	2.98	0.3	0.42	14	30	54	-0.5	1.5	0.9	0.6	18	193	0.6	1	6	-0.2	2.4	8
GA2	L15-00109	L15-00111	436526	7419189	1-0.5 mm	4	20	29	3.78	606	0.71	80	3.2	0.46	0.52	16	35	58	-0.5	2	0.9	0.6	20	196	0.6	1	6	-0.2	2.9	7.5
GA2	L15-00132	L15-00112	436526	7419189	0.5-0.25 mm	3	20	29	3.67	550	0.68	100	3.18	0.52	0.53	14	30	57	-0.5	2.5	0.8	0.6	22	190	0.6	-1	6	-0.2	3.1	4.5
GA2	L15-00110	L15-00113	436526	7419189	0.25 mm-75mm	4	30	28	3.12	390	0.56	80	2.16	0.49	0.54	12	35	46	-0.5	1	0.8	0.4	17	138	0.4	-1	5	-0.2	3	5
GA2	L15-00120	L15-00114	436526	7419189	<75 mm	7	30	32	3.69	427	0.72	120	2.3	0.63	0.74	16	35	60	-0.5	3.5	0.8	0.4	19	158	0.6	-1	5	-0.2	3.7	5
GA3	L15-00148	L15-00115	436516	7419189	bulk <6 mm	3	10	28	3.64	537	0.94	60	2.5	0.57	0.95	20	35	70	-0.5	1.5	0.8	0.6	19	145	0.6	2	5	-0.2	2.15	4.5
GA3	L15-00126	L15-00116	436516	7419189	6-2 mm	2	10	19	2.7	492	0.62	40	2.14	0.47	0.48	14	25	47	-0.5	1	0.8	0.6	13	127	0.6	2	4	-0.2	1.45	7.5
GA3	L15-00130	L15-00117	436516	7419189	2-1 mm	-1	-10	22	3.8	620	0.96	40	3.46	0.58	0.65	16	25	68	-0.5	0.5	0.9	0.6	18	207	0.6	1	7	-0.2	2	8.5
GA3	L15-00134	L15-00118	436516	7419189	1-0.5 mm	2	-10	26	3.87	634	1.06	60	3.5	0.68	0.86	18	30	74	-0.5	1.5	0.7	0.6	22	200	0.6	1	7	-0.2	2.7	6
GA3	L15-00117	L15-00119	436516	7419189	0.5-0.25 mm	2	10	32	3.88	622	1.01	120	3.24	0.81	0.91	20	30	73	-0.5	2	0.7	0.6	23	185	0.6	1	6	-0.2	2.5	6.5
GA3	L15-00169	L15-00120	436516	7419189	0.25 mm-75mm	3	10	24	3.04	428	0.79	80	1.9	0.57	0.88	16	30	56	-0.5	1	0.5	0.4	19	116	0.4	1	4	-0.2	1.9	5
GA3	L15-00103	L15-00121	436516	7419189	<75 mm	10	20	35	3.82	468	1.07	120	2.11	0.57	1.4	24	45	76	-0.5	2.5	0.7	0.4	26	158	0.4	2	4	-0.2	2.7	4
GA4	L15-00116	L15-00122	436496	7419189	bulk <6 mm	-1	10	18	3.49	483	0.72	60	2.92	0.74	0.45	12	25	65	-0.5	2	0.5	0.6	17	172	0.4	1	6	-0.2	3.2	6
GA4	L15-00156	L15-00123	436496	7419189	6-2 mm	23	10	12	2.62	407	0.62	40	2.77	0.34	0.23	6	15	48	-0.5	1	0.6	0.6	11	168	0.6	-1	6	-0.2	2.25	6.5
GA4	L15-00129	L15-00124	436496	7419189	2-1 mm	-1	10	13	3.52	606	0.9	40	3.9	0.42	0.33	8	15	70	-0.5	0.5	0.4	0.6	15	250	0.6	2	8	-0.2	2.8	6
GA4	L15-00138	L15-00125	436496	7419189	1-0.5 mm	2	10	16	3.3	546	0.77	40	3.69	0.6	0.39	10	15	83	-0.5	2	0.4	0.6	19	208	0.6	2	7	-0.2	3.3	5
GA4	L15-00151	L15-00126	436496	7419189	0.5-0.25 mm	1	10	15	3	468	0.66	60	3.68	0.75	0.44	8	20	62	-0.5	1	0.4	0.6	18	177	0.4	-1	5	-0.2	3.2	4
GA4	L15-00159	L15-00127	436496	7419189	0.25 mm-75mm	1	10	15	2.94	396	0.59	40	2.4	0.87	0.54	10	20	55	-0.5	1.5	0.4	0.4	17	126	0.4	-1	4	-0.2	2.8	4.5
GA4	L15-00106	L15-00128	436496	7419189	<75 mm	8	20	19	3.75	502	0.75	80	2.32	0.95	0.74	14	35	79	-0.5	0.5	0.6	0.6	24	179	0.4	2	6	-0.2	4.55	4
GA5	L15-00137	L15-00129	436446	7419189	bulk <6 mm	1	10	15	3.3	514	0.67	40	2.92	0.56	0.99	6	15	86	-0.5	1	0.6	0.8	89	222	0.6	1	6	-0.2	3.4	3.5
GA5	L15-00111	L15-00130	436446	7419189	6-2 mm	1	-10	13	2.41	441	0.49	20	2.38	0.44	0.7	4	10	79	-0.5	-0.5	0.5	0.6	72	205	0.4	1	5	-0.2	2.75	5.5
GA5	L15-00140	L15-00131	436446	7419189	2-1 mm	-1	-10	13	2.77	571	0.56	20	2.77	0.51	0.75	6	10	91	-0.5	1.5	0.5	0.8	85	222	0.6	-1	5	-0.2	2.9	4
GA5	L15-00157	L15-00132	436446	7419189	1-0.5 mm	2	20	13	2.81	507	0.59	60	2.81	0.49	0.81	6	15	89	-0.5	1.5	0.5	0.6	83	212	0.4	-1	5	-0.2	3.1	4.5
GA5	L15-00146	L15-00133	436446	7419189	0.5-0.25 mm	1	20	18	3.2	543	0.65	80	3.72	0.57	0.99	8	15	84	-0.5	1.5	0.6	0.8	102	263	0.6	1	6	-0.2	3.65	3
GA5	L15-00135	L15-00134	436446	7419189	0.25 mm-75mm	-1	30	14	3.2	484	0.64	60	2.65	0.57	1.02	8	20	88	-0.5	1	0.6	0.6	84	192	0.4	1	5	-0.2	3.25	2.5
GA5	L15-00125	L15-00135	436446	7419189	<75 mm	3	30	17	3.89	563	0.74	100	2.21	0.75	1.46	10	25	93	-0.5	2	0.6	0.6	91	191	0.4	2	6	-0.2	4.4	4.5
GA6	L15-00114	L15-00136	436546	7419189	bulk <6 mm	48	30	32	3.61	350	1.32	140	2.65	0.16	5.57	20	55	75	-0.5	5	0.8	0.4	30	179	2	1	3	-0.2	3.25	5
GA6	L15-00143	L15-00137	436546	7419189	6-2 mm	12	20	31	2.43	234	1.21	120	2.96	0.09	7	18	35	64	-0.5	6	0.9	0.6	25	170	3	-1	2	-0.2	2.6	4
GA6	L15-00112	L15-00138	436546	7419189	2-1 mm	16	20	31	2.38	303	1.22	140	3.01	0.09	5.86	18	35	61	-0.5	3.5	0.9	0.6	26	185	2.6	-1	2	-0.2	2.5	5
GA6	L15-00149	L15-00139	436546	7419189	1-0.5 mm	42	20	37	3.49	371	1.49	160	3.47	0.14	5.85	22	50	83	-0.5	5.5	0.9	0.6	33	206	2.6	2	3	-0.2	3.25	4
GA6	L15-00133	L15-00140	436546	7419189	0.5-0.25 mm	52	30	34	3.46	335	1.41	160	3.72	0.16	5.41	20	50	76	-0.5	5	0.8	0.6	32	206	2	-1	3	-0.2	3.25	3.5
GA6	L15-00127	L15-00141	436546	7419189	0.25 mm-75mm	29	30	31	3.97	372	1.23	140	2.38	0.18	5.45	20	55	75	-0.5	4	0.7	0.4	33	187	1.8	1	4	-0.2	3.25	3.5
GA6	L15-00144	L15-00142	436546	7419189	<75 mm	58	30	38	4.6	410	1.33	180	1.82	0.22	5.93	22	75	91	-0.5	5	0.8	0.4	35	176	1.6	1	4	-0.2	3.7	3.5
GA7	L15-00136	L15-00143	436556	7419189	bulk <6 mm	147	30	26	3.87	374	1.55	220	2.04	0.15	6.49	22	45	93	-0.5	4	0.6	0.4	28	166	1.6	1	3	-0.2	2.4	3.5
GA7	L15-00104	L15-00144	436556	7419189	6-2 mm	26	20	21	2.12	253	1.25	180	1.69	0.08	8.99	16	30	56	-0.5	3	0.6	0.6	21	119	2	1	2	-0.2	2.8	4
GA7	L15-00139	L15-00145	436556	7419189	2-1 mm	22	20	26	2.66	295	1.58	200	2.66	0.09	8.17	18	35	70	-0.5	5.5	0.6	0.6	23	148	2	-1	2	-0.2	1.8	4
GA7	L15-00113	L15-00146	436556	7419189	1-0.5 mm	35	30	28	3.37	383	1.65	220	2.53	0.12	5.59	24	45	85	-0.5	3.5	0.6	0.6	26	172	1.6	1	3	-0.2	2.3	4.5
GA7	L15-00121	L15-00147	436556	7419189	0.5-0.25 mm	41	30	31	3.84	431	1.83	260	2.92	0.16	5.64	24	50	94	-0.5	4	0.6	0.6	30	194	1.6	1	3	-0.2	2.6	5.5
GA7	L15-00105	L15-00148	436556	7419189	0.25 mm-75mm	35	30	27	4.26	387	1.54	200	2.02	0.16	5.62	26	55	92	-0.5	3	0.5	0.4	30	181	1.2	1	3	-0.2	2.75	4.5
GA7	L15-00122	L15-00149	436556	7419189	<75 mm	71	30	38	6.16	498	2.34	300	2.57	0.24	7.51	32	80	151	-0.5	5	0.7	0.6	37	247	1.6	1	4	-0.2	3.75	5.5
GA8	L15-00152	L15-00150	436576	7419189	bulk <6 mm	140	40	27	4.66	484	0.88	80	2.45	0.24	2.18	22	50	78	-0.5	2.5	1	0.4	27	169	1	1	4	-0.2	2.3	4.5
GA8	L15-00155	L15-00151	436576	7419189	6-2 mm	31	40	20	3.29	343	0.67	40	2.16	0.18	0.77	16	40	59	-0.5	2	1.6	0.6	15	119	1.2	-1	3	-0.2	1.2	9
GA8	L15-00107	L15-00152	436576	7419189	2-1 mm	82	40	33	4.72	552	0.93	80	2.98	0.34	1.34	22	45	83	-0.5	3	1.5	0.8	25	202	1.6	1	4	-0.2	2.35	9
GA8	L15-00119	L15-00153	436576	7419189	1-0.5 mm	183	50	31	5.1	583	1.05	100	2.94	0.32	2.12	24	50	91	-0.5	2.5	0.9	0.4	25	184	1	-1	3	-0.2	2.5	5
GA8	L15-00108	L15-00154	436576	7419189	0.5-0.25 mm	151	40	36	5.08	567	1.02	120	3.05	0.31	2.17	26	50	85	-0.5	1.5	0.9	0.6	28	215	1.2	1	4	-0.2	2.7	5
GA8	L15-00164	L15-00155	436576	7419189	0.25 mm-75mm	120	40	26	4.61	450	0.88	80	2.17	0.26	2.64	20	50	77	-0.5	2.5	0.6	0.4	25	143	0.8	1	4	-0.2	2.4	4.5
GA8	L15-00142	L15-00156	436576	7419189	<75 mm	218	40	33	5.47	478	1.08	120	2.07	0.3	2.65	22	60	97	-0.5	3	0.7	0.6	26	154	0.8	1	4	-0.2	3.05	3
GA9	L15-00131	L15-00157	436626	7419189	bulk <6 mm	-1	10	22	5.34	966	1.18	40	1.93	1.25	1.45	12	20	79	-0.5	2	0.8	0.6	19	125	0.4	-1	7	-0.2	2.5	4
GA9	L15-00160	L15-00158	436626	7419189	6-2 mm	-1	-10	35	4.94	894	1.19	20	1.89	1.08	1.03	12	20	80	-0.5	4.5	0.6	0.6	19	114	0.4	-1	6	-0.2	1.8	5.5
GA9	L15-00118	L15-00159	436626	7419189	2-1 mm	-1	-10	31	6.29	1280	1.42	40	2.39	1.48	1.28	12	15	97	-0.5	2	1.1	0.6	20	142	0.4	1	7	-0.2	2.6	6
GA9	L15-00165	L15-00160	436626	7419189	1-0.5 mm	-1	-10	26	5.96	1340	1.34	40	2.21	1.61	1.23	12	20	92	-0.5	2	1	0.6	21	143	0.4	1	7	-0.2	2.6	6.5
GA9	L15-00162	L15-00161	436626	7419189	0.5-0.25 mm	-1	-10	22	4.82	1020	1.12	40	1.88	2.04	1.2	10	20	73	-0.5	1.5	0.9	0.4	20	121	0.2	1	6	-0.2	2.35	9
GA9	L15-00147	L15-00162	436626	7419189	0.25 mm-75mm	-1	-10	21	4.49	757	1.01	60	1.47	1.05	1.46	16	20	63	-0.5	1	0.8	0.4	20	104	0.2	-1	6	0.2	2.35	2.5
GA9	L15-00101	L15-00163	436626	7419189	<75 mm	13	30	26	4.82	602	1.31	100	1.47	0.93	1.37	14	25	76	-0.5	0.5	0.9	0.4	23	118	0.2	2	6	-0.2	3.35	3.5

APPENDIX 4

STANDARDS

APPENDIX 4 - CSIRO weathered rock standards

Element	Units	Standard 6 Preferred value	Standard 6 Analysis 1	Standard 6 Analysis 2	Standard 9 Preferred value	Standard 9 Analysis 1	Standard 9 Analysis 2	Standard 10 Preferred value	Standard 10 Analysis 1	Standard 10 Analysis 2
Au	ppb	86	84	91	87	89	115	31	30	28
Hg	ppb	?	<10	10	?	60	60	?	20	20
Cu	ppm	6	8	8	141	150	146	31	27	29
Fe2O3	%	0.42	0.6	0.6	65.05	68.63	67.91	10.94	10.82	10.99
Mn	ppm	8	18	18	1543	1780	1680	348	341	349
MgO	%	0.31	0.33	0.3	0.15	0.15	0.13	0.68	0.61	0.65
S	%	0.016	0.014	0.014	0.041	0.038	0.038	0.144	0.1	0.11
K2O	%	3.54	3.67	3.84	0.2	0.18	0.17	0.2	0.22	0.23
Na2O	%	0.4	0.42	0.42	0.04	0.04	0.04	0.15	0.19	0.19
CaO	%	0.03	0.04	0.03	0.13	0.14	0.1	20.03	20	20.57
Ni	ppm	9	12	10	30	44	48	135	120	124
Cr	ppm	120	30	50	471	450	445	122	115	120
Zn	ppm	5	11	10	295	336	340	12	14	14
Ag	ppm	0.45	<0.5	<0.5	0.83	0.5	0.5	0.54	<0.5	<0.5
As	ppm	2	1	1.5	438	440	435	20	21.5	21.5
Bi	ppm	0.3	0.2	0.2	1.32	1.1	1.1	0.31	0.3	0.3
Mo	ppm	3	0.6	0.6	5	4.6	4.4	3	1.4	1.6
Pb	ppm	10	13	13	53	48	47	4	6	6
Rb	ppm	109	98.5	99.8	6	4.42	4.64	6	5.38	5.36
Sb	ppm	12.8	6.8	7	0.6	0.8	0.8	0.4	0.2	0.2
Se	ppm	2	<1	<1	3	2	2	3	1	1
Sn	ppm	0.75	<1	<1	1.12	<1	<1	1.32	1	1
Te	ppm	?	<0.2	<0.2	?	0.4	0.4	?	<0.2	<0.2
U	ppm	1	1.1	1.15	1	2.2	2.15	1	1.3	1.35
W	ppm	6	3	3	9	11.5	12	3	2.5	3

APPENDIX 5

DIGITAL DATA DISC